Reactions of some Decaosmium Clusters with Electrophilic and Nucleophilic Reagents: *X*-Ray Structure Analyses of $[N(PPh_3)_2][Os_{10}C(CO)_{24}(\mu\text{-}I)]$, $[Os_{10}C(CO)_{24}(\mu\text{-}I)_2]$, $[N(PPh_3)_2]_2[Os_{10}C(CO)_{22}(NO)I]$, $[Os_{10}C(CO)_{23}\{P(OMe)_3\}(\mu\text{-}I)_2]$ and of Two Isomers of $[Os_{10}C(CO)_{21}\{P(OMe)_3\}_4]$†

Robert J. Goudsmit, Peter F. Jackson, Brian F. G. Johnson, Jack Lewis,* William J. H. Nelson, José Puga, and Maria D. Vargas
University Chemical Laboratory, Lensfield Road, Cambridge CB2 1EW
Dario Braga, Kim Henrick, Mary McPartlin,* and Angelo Sironi
School of Chemistry, The Polytechnic of North London, London N7 8DB

The carbido-dianion $[Os_{10}C(CO)_{24}]^{2-}$ (**1**) reacts with halogens X_2 to give firstly $[Os_{10}C(CO)_{24}(\mu\text{-}X)]^-$, and then $[Os_{10}C(CO)_{24}(\mu\text{-}X)_2]$ (X = Cl, Br, or I). The dianion (**1**) is regenerated on treatment of $[Os_{10}C(CO)_{24}(\mu\text{-}X)]^-$ or $[Os_{10}C(CO)_{24}(\mu\text{-}X)_2]$ with the nucleophiles X^-, OH^-, PR_3 (R = OMe or C_6H_5), C_5H_5N, MeCN, or CO in polar solvents (tetrahydrofuran, methanol, acetone, or dichloromethane). Treatment of $[Os_{10}C(CO)_{24}(\mu\text{-}I)_2]$ (**3**) with $[N(PPh_3)_2][NO_2]$ in dichloromethane gives the nitrosyl dianion $[Os_{10}C(CO)_{22}(NO)I]^{2-}$ (**4**). With an excess of $P(OMe)_3$ in xylene, complex (**3**) gives a mixture of products from which the phosphite-containing clusters $[Os_{10}C(CO)_{23}\{P(OMe)_3\}(\mu\text{-}I)_2]$ (**5**) and $[Os_{10}C(CO)_{21}\{P(OMe)_3\}_4]$ (**6**) were separated and identified. The neutral species (**5**) was shown to react with an iodide ion, in a similar manner to the reaction shown by (**3**), to sequentially remove the bridging iodine ligands with formation of the dianion $[Os_{10}C(CO)_{23}\{P(OMe)_3\}]^{2-}$ (**5b**). An isomer of the cluster (**6**), compound (**6a**), was prepared by the reaction of $[Os_{10}H_2C(CO)_{24}]$ with $P(OMe)_3$ in xylene. Crystal-structure analyses of complexes $[N(PPh_3)_2][Os_{10}C(CO)_{24}(\mu\text{-}I)]$, (**3**), (**4**), (**5**), (**6**), and (**6a**) are reported and the possible mechanisms for their formation together with a discussion of the factors affecting the reactivity of the Os_{10} series to nucleophiles are reported.

The synthesis and characterisation of a number of high nuclearity transition-metal clusters species have been reported. However, comparatively little is known of the factors which affect their reactions towards nucleophilic and electrophilic reagents. It has been previously shown that most clusters of ruthenium and osmium containing six or less metal atoms undergo reaction with nucleophiles to give initially simple adducts. Under more forcing conditions, these adducts react further and either metal–metal bond cleavage or carbonyl expulsion may occur leading eventually to cluster breakdown.[1] In contrast, large clusters containing interstitial atoms appear to be resistant to such fragmentation. An additional factor which may affect the chemistry of high nuclearity clusters is whether or not the structure is capped. In general, nucleophilic addition to capped clusters occurs preferentially at the capping atom(s) which may be regarded as the site of electron deficiency. This process is exemplifed by the reactions of $[Os_n(CO)_m]$ (n = 6 or 7, m = 18 or 21) with OH^- which leads to the formation of the more symmetric dianions $[Os_{n-1}(CO)_{m-1}]^{2-}$ *via* a decapping process.[2] For the tetracapped $[Os_{10}C(CO)_{24}]^{2-}$ a remarkable resistance to attack by nucleophiles such as OH^-, CO, and PR_3 has been observed;[3] this is most probably due to the presence of the negative charge on the cluster. However, $[Os_{10}C(CO)_{24}]^{2-}$ does react with a variety of electrophiles, *i.e.* H^+,[4] $[Au(PR_3)]^+$(R = Ph or OEt),[5] $[Cu(NCMe)]^+$,[5] and NO^+.[6]

Here we report studies of the reactions of the dianion $[Os_{10}C(CO)_{24}]^{2-}$ (1) with halogens X_2 (X = Cl, Br, or I) which may be regarded as occurring *via* the electrophilic addition of X^+ to the anionic cluster. We have also examined the chemistry of some of the products of these reactions, *viz.* $[Os_{10}C(CO)_{24}(\mu\text{-}I)]^-$ (2) and $[Os_{10}C(CO)_{24}(\mu\text{-}I)_2]$ (3) and have observed that they show an enhanced reactivity towards nucleophiles such as PR_3. This is thought to be due not only to the reduction in charge of the species but probably also to the opening up of the molecule brought about by the introduction of the bridging halide ligands.

Results and Discussion

Reactions of $[Os_{10}C(CO)_{24}]^{2-}$ (1) *with Halogens.*—We have recently demonstrated that a number of anionic carbonyl clusters of osmium undergo reaction with iodine (I_2) either by oxidation of the cluster with concomitant rearrangement of the metal skeleton or by the direct electrophilic addition of iodine as I^+ to the cluster framework.[7] In the latter case the iodine atom(s) may adopt a terminal or bridging bonding mode to the cluster core. Thus, for example as summarised in Table 1, the dianion $[Os_6(CO)_{18}]^{2-}$ is oxidised to $[Os_6(CO)_{18}]$ while the anions $[Os_4H_3(CO)_{12}]^-$, $[Os_5(CO)_{15}]^{2-}$, and [Os$_8$H-

---

† Bis(triphenylphosphine)iminium μ_6-carbido-tetracosacarbonyl-μ-iodo-*polyhedro*-decaosmate(1 −), μ_6-carbido-tetracosacarbonyl-di-μ-iodo-*polyhedro*-decaosmium, bis[bis(triphenylphosphine)iminium] μ_6-carbido-docosacarbonyl(iodo)nitrosyl-*polyhedro*-decaosmate(2 −), μ_6-carbido-tricosacarbonyl-di-μ-iodo-(trimethyl phosphite)-*polyhedro*-decaosmium, μ_6-carbido-μ_3-carbonyl-icosacarbonyl-tetrakis-(trimethyl phosphite)-*polyhedro*-decaosmium, and μ_6-carbido-μ-carbonyl-icosacarbonyl-tetrakis(trimethyl phosphite)-*polyhedro*-decaosmium respectively.

Supplementary data available (No. SUP 56252, 75 pp.): thermal parameters, H-atom co-ordinates for (2), full lists of bond lengths and angles. See Instructions for Authors, *J. Chem. Soc., Dalton Trans.*, 1985, Issue 1, pp. xvii—xix. Structure factors are available from the editorial office.

Non-S.I. unit employed: atm ≈ 13.6 × 9.8 Pa.

Preliminary report: D. H. Farrar, P. F. Jackson, B. F. G. Johnson, J. Lewis, W. J. H. Nelson, M. D. Vargas, and M. McPartlin, *J. Chem. Soc., Chem. Commun.*, 1981, 1009.

Table 1. Modes of reaction of $\mathrm{I_2}$ with clusters

Reactant	Product	Ref.
(*i*) Oxidation/rearrangement		
$[\mathrm{Os_6(CO)_{18}}]^{2-}$	$[\mathrm{Os_6(CO)_{18}}]$	7*a*
(*ii*) $\mathrm{I^+}$ Addition/bond cleavage		
$[\mathrm{Os_4H_3(CO)_{12}}]^-$	$[\mathrm{Os_4H_3(CO)_{12}(\mu\text{-}I)}]$	7*b*
$[\mathrm{Os_{10}C(CO)_{24}}]^{2-}$	$[\mathrm{Os_{10}C(CO)_{24}(\mu\text{-}I)}]^-$	
$[\mathrm{Os_{10}C(CO)_{24}(\mu\text{-}I)}]^-$	$[\mathrm{Os_{10}C(CO)_{24}(\mu\text{-}I)_2}]$	
(*iii*) $\mathrm{I^+}$ Addition/no major change in cluster geometry		
$[\mathrm{Os_5(CO)_{15}}]^{2-}$	$[\mathrm{Os_5(CO)_{15}I}]^-$	7*c*
(*iv*) $\mathrm{I^+}$ Addition/bond cleavage/rearrangement		
$[\mathrm{Os_8H(CO)_{22}}]^-$	$[\mathrm{Os_8H(CO)_{22}(\mu\text{-}I)}]$	7*d*

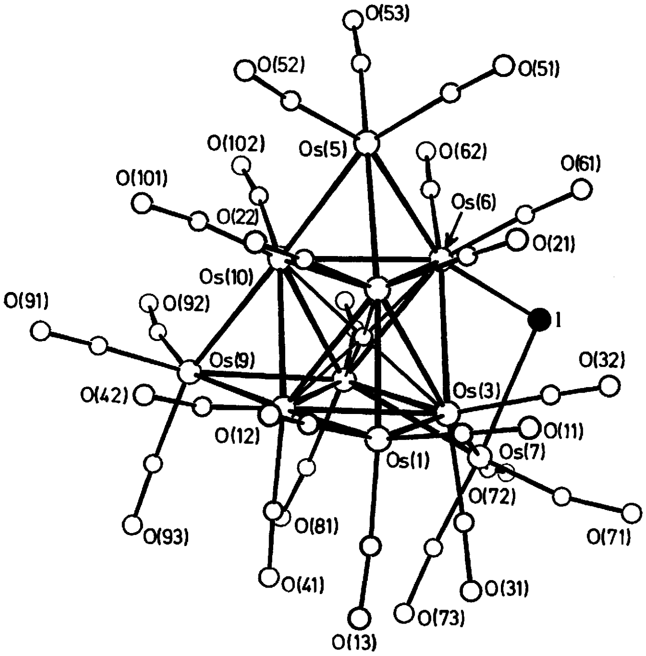

Figure 1. Structure of $[\mathrm{Os_{10}C(CO)_{24}(\mu\text{-}I)}]^-$ (**2**); the numbering of the carbon atoms corresponds to that of the relevant carbonyl oxygen atoms. The first digit(s) of each oxygen or carbon atom is the number of the osmium atom to which the group is attached

$\mathrm{(CO)_{22}]^-}$ form the addition products $[\mathrm{Os_4H_3(CO)_{12}(\mu\text{-}I)}]$, $[\mathrm{Os_5(CO)_{15}I}]^-$, and $[\mathrm{Os_8H(CO)_{22}(\mu\text{-}I)}]$ respectively.

The salts $[\mathrm{Y}]_2[\mathrm{Os_{10}C(CO)_{24}}]$ (**1**) $\{\mathrm{Y} = [\mathrm{N(PPh_3)_2}]^+$, $[\mathrm{PMePh_3}]^+$, or $[\mathrm{AsPh_4}]^+\}$ react with $\mathrm{I_2}$ (slightly more than two equivalents) in dichloromethane to give the corresponding salts of the new anion $[\mathrm{Os_{10}C(CO)_{24}(\mu\text{-}I)}]^-$ (**2**). Addition of two further equivalents of $\mathrm{I_2}$ gives the neutral species $[\mathrm{Os_{10}C(CO)_{24}(\mu\text{-}I)_2}]$ (**3**), as shown in equation (i). Both species

$$\begin{tikzcd}
{[\mathrm{Os_{10}C(CO)_{24}}]^{2-}} \arrow[r, "2\mathrm{I_2}"] & {[\mathrm{Os_{10}C(CO)_{24}(\mu\text{-}I)}]^- + \mathrm{I_3}^-} \arrow[d, "2\mathrm{I_2}"] \\
 & {[\mathrm{Os_{10}C(CO)_{24}(\mu\text{-}I)_2}] + \mathrm{I_3}^-}
\end{tikzcd} \qquad \text{(i)}$$

(**2**) and (**3**) were produced in high yields and were characterised on the basis of analytical and spectroscopic data (Table 2).

Table 2. Infrared carbonyl [nitrosyl] stretching frequencies *

Complex		ν(CO)[ν(NO)]/cm^{-1}
(*i*) Reaction of (**1**) with halogens		
$[\mathrm{Os_{10}C(CO)_{24}}]^{2-}$	(**1**)	2 033s, 1 986s
$[\mathrm{Os_{10}C(CO)_{24}(\mu\text{-}Cl)}]^-$		2 067s, 2 057vs, 2 022m, 2 008s
$[\mathrm{Os_{10}C(CO)_{24}(\mu\text{-}Br)}]^-$		2 066s, 2 056vs, 2 020m, 2 006s
$[\mathrm{Os_{10}C(CO)_{24}(\mu\text{-}I)}]^-$	(**2**)	2 065s, 2 057vs, 2 017m, 2 004s
$[\mathrm{Os_{10}C(CO)_{24}(\mu\text{-}Cl)_2}]$		2 087s, 2 079s, 2 045vs, 2 032s, 2 016w (sh)
$[\mathrm{Os_{10}C(CO)_{24}(\mu\text{-}Br)_2}]$		2 085s, 2 077m, 2 040s, 2 029m, 2 013w (sh)
$[\mathrm{Os_{10}C(CO)_{24}(\mu\text{-}I)_2}]$	(**3**)	2 084vs, 2 076m, 2 038s, 2 027m, 2 011w (sh)
(*ii*) Reaction of (**3**) with $[\mathrm{N(PPh_3)_2}][\mathrm{NO_2}]$		
$[\mathrm{Os_{10}C(CO)_{22}(NO)I}]^{2-}$	(**4**)	2 072w, 2 042vs, 2 004s, 1 993m (sh), [1 724w]
	(**4a**)	2 092w, 2 067vs, 2 030m (sh), 2 019s
	(**4b**)	2 090w, 2 064vs, 2 025m, 2 010s
(*iii*) Reaction of (**3**) with $\mathrm{P(OMe)_3}$		
$[\mathrm{Os_{10}C(CO)_{21}\{P(OMe)_3\}_4}]$	(**6**)	2 058w, 2 023vs, 2 003m (sh)
$[\mathrm{Os_{10}C(CO)_{21}\{P(OMe)_3\}_4}]$	(**6a**)	2 056 (sh), 2 019s, 1 929 (sh), 1 730w
	(**7**)	2 053vw, 2 022vs, 2 002m (sh)
	(**8**)	2 079w, 2 046m, 2 028 (sh), 2 010m (sh)
	(**8a**)	2 069vw, 2 036m, 2 018s (sh), 2 009vs, 1 983s, 1 969 (sh)
	(**9**)	2 089m, 2 069vs, 2 051m, 2 034vs, 2 012s
	(**10**)	2 098vs, 2 089w, 2 075 (sh), 2 066m, 2 032vs, 2 022s (sh), 1 989w (sh)
$[\mathrm{Os_{10}C(CO)_{23}\{P(OMe)_3\}\text{-}(\mu\text{-}I)_2}]$	(**5**)	2 099w, 2 080vs, 2 074s (sh), 2 043m (sh), 2 033s, 2 020m (sh), 1 987w (sh), 1 974w, 1 941w (sh)
	(**5a**)	2 082w, 2 053vs, 2 025m, 2 015m (sh), 2 001m
	(**5b**)	2 075w, 2 046vs, 2 029vs, 2 018s, 2 003vs, 1 983m (sh)

* In $\mathrm{CH_2Cl_2}$ and anions as the $[\mathrm{N(PPh_3)_2}]^+$ salts, except for compounds (**8a**), (**5a**), and (**5b**) which were recorded in acetone as the $[\mathrm{NBu^i{}_4}]^+$ salts.

Where $\mathrm{Y} = [\mathrm{N(PPh_3)_2}]^+$ the only other product isolated from the reaction was the salt $[\mathrm{N(PPh_3)_2}][\mathrm{I_3}]$.

Dark brown crystals of the $[\mathrm{N(PPh_3)_2}]^+$ salt of (**2**) and the complex (**3**), suitable for *X*-ray analysis were grown over a period of 4 and 2 d respectively at 25 °C from dichloromethane–methanol by slow evaporation. The molecular structures of (**2**) and (**3**) are shown in Figures 1 and 2 respectively. Some important bond distances and angles are given in Table 3.

The analyses reveal that attack by $\mathrm{I^+}$ leads to an opening out of a capping tetrahedron through breaking of an Os–Os bond accompanied by bending back of an $\mathrm{Os(CO)_3}$ hinged unit within the $\mathrm{Os_{10}}$ skeleton. Whereas it has been shown that nucleophilic attack in capped clusters apparently occurs preferentially at a capping atom, the centre of electron deficiency, the site of electrophilic attack is less easily defined and may not necessarily be the same for a range of electrophiles. Our studies on the electrophilic addition of $\mathrm{NO^+}$ to $[\mathrm{Os_{10}C\text{-}(CO)_{24}}]^{2-}$ (**1**)[6] strongly suggest that the attack occurs at an Os–Os bond. The product of this reaction, $[\mathrm{Os_{10}C(CO)_{24}}$-

Table 3. Selected bond lengths (Å) and angles (°) for $[Os_{10}C(CO)_{24}(\mu\text{-}I)]^-$ (**2**), $[Os_{10}C(CO)_{24}(\mu\text{-}I)_2]$ (**3**), and $[Os_{10}C(CO)_{23}\{P(OMe)_3\}(\mu\text{-}I)_2]$ (**5**)*

	(2)	**(3)**	**(5)**
(*i*) Bond lengths			
Os–Os within octahedron			
2–3	2.867(3)	2.832(4)	2.825(2)
2–4	2.863(3)	2.893(4)	2.886(2)
2–6	2.884(2)	2.883(4)	2.884(2)
2–10	2.844(2)	2.837(4)	2.842(2)
3–4	2.879(2)	2.897(4)	2.902(2)
3–6	2.997(2)	2.950(4)	2.942(2)
3–8	3.003(2)	2.957(4)	2.936(2)
4–8	2.880(2)	2.941(4)	2.921(2)
4–10	2.872(2)	2.949(4)	2.963(2)
6–8	2.986(3)	2.915(4)	2.943(3)
6–10	2.875(2)	2.896(4)	2.881(2)
8–10	2.881(3)	2.980(4)	3.001(2)
Mean	2.901(2)	2.911(4)	2.910(2)
Os–Os from capping atoms (* denotes an 'open cap')			
1–2	2.790(2)	2.753(4)	2.745(2)
1–3	2.807(3)	2.752(4)	2.755(2)
1–4	2.767(2)	2.878(4)	2.858(2)
2–5	2.769(2)	2.740(4)	2.747(2)
3–7	*2.844(3)	*2.823(4)	*2.825(2)
4–9	2.770(2)		
5–6	2.853(2)	2.851(4)	2.843(2)
5–10	2.766(3)	2.767(4)	2.753(2)
7–8	*2.836(2)	*2.833(4)	*2.817(2)
8–9	2.823(2)	*2.826(4)	*2.897(2)
9–10	2.785(3)	*2.835(4)	*2.851(2)
Os–iodine			
4–I(2)		2.737(5)	2.738(3)
6–I(1)	2.717(4)	2.730(5)	2.724(3)
7–I(1)	2.730(4)	2.746(6)	2.737(4)
9–I(2)		2.732(6)	2.733(3)
Os–carbido C			
Range	2.03(4)—2.07(4)	1.93(7)—2.22(7)	2.00(3)—2.13(3)
Mean	2.05(4)	2.07(7)	2.06(3)
Os–carbonyl C			
Range	1.69(5)—1.92(5)	1.73(7)—2.14(7)	1.80(4)—1.95(4)
Mean	1.847(5)	1.843(7)	1.869(4)
Os–P			2.254(12)
Carbonyl C–O			
Range	1.05(7)—1.31(7)	1.01(9)—1.33(9)	1.09(4)—1.27(4)
Mean	1.17(7)	1.21(9)	1.15(4)
(*ii*) Bond angles			
Os(4)–I(2)–Os(9)		91.0(2)	91.9(1)
Os(6)–I(1)–Os(7)	91.7(1)	90.3(2)	90.5(1)
I(1)–Os(6)–Os(2)	139.3(1)	136.9(2)	137.7(1)
I(1)–Os(6)–Os(3)	82.8(1)	82.2(1)	82.8(1)
I(1)–Os(6)–Os(5)	157.8(1)	155.3(2)	155.4(1)
I(1)–Os(6)–Os(8)	82.1(1)	84.2(1)	83.6(1)
I(1)–Os(6)–Os(10)	138.5(1)	144.1(2)	143.3(1)
I(1)–Os(7)–Os(3)	85.1(1)	84.3(1)	84.7(1)
I(1)–Os(7)–Os(8)	84.7(1)	85.5(1)	85.8(1)
I(2)–Os(4)–Os(1)		157.4(1)	156.9(1)
I(2)–Os(4)–Os(2)		137.0(1)	135.0(1)
I(2)–Os(4)–Os(3)		142.3(1)	144.0(1)
I(2)–Os(4)–Os(8)		83.2(1)	84.4(1)
I(2)–Os(4)–Os(10)		81.6(1)	80.2(1)
I(2)–Os(9)–Os(8)		85.5(1)	85.0(1)
I(2)–Os(9)–Os(10)		83.8(1)	82.3(1)
P–Os(9)–Os(8)			167.8(3)
P–Os(9)–Os(10)			105.1(3)
P–Os(9)–I(2)			91.3(3)
Os–carbido C–Os			
cis			
Range	87(1)—94(1)	80(3)—100(3)	86(1)—94(1)
Mean	90(1)	89(3)	90(1)
trans			
Range	175(1)—176(1)	166(3)—169(3)	171(2)—177(2)
Mean	176(1)	168(1)	174(2)
Carbonyl–Os–carbonyl			
At capping Os atoms			
Range	88(2)—99(2)	85(3)—97(3)	90(2)—96(2)
Mean	92(2)	90(3)	92(2)
At Os atoms of octahedron			
Range	90(2)—95(2)	84(7)—99(3)	89(2)—101(2)
Mean	93(2)	92(3)	95(2)
Os–C–O (carbonyl)			
Range	163(5)—178(5)	155(5)—178(5)	166(4)—180(4)
Mean	173(5)	169(5)	173(4)

* Here, and in Tables 4 and 5, the values in parentheses for the mean bond lengths are the mean of the individual estimated standard deviations.

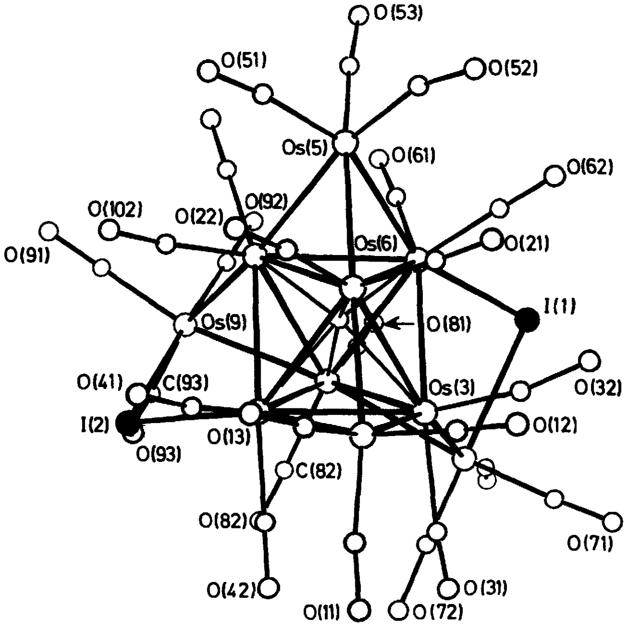

Figure 2. Structure of $[Os_{10}C(CO)_{24}(\mu\text{-}I)_2]$ (**3**) (see Figure 1 for numbering scheme)

$(\mu\text{-}NO)]^-$, contains a bridging NO ligand and is similar in core geometry to the products of the halogen reaction.

The reaction of the dianion (**1**) with two or four equivalents of Br_2 (fresh, dilute solutions of Br_2 in dichloromethane) also gives

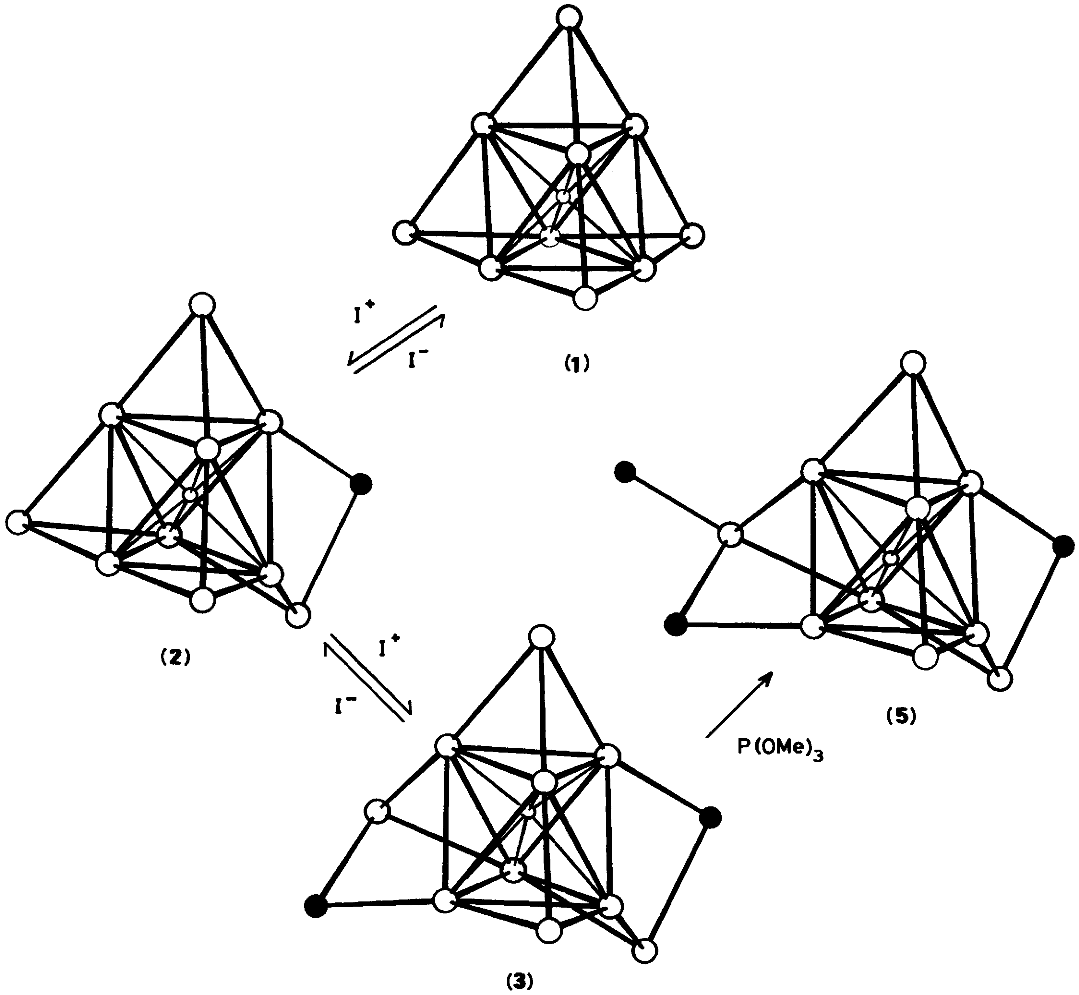

Figure 3. Relationship between the cluster cores in $[Os_{10}C(CO)_{24}]^{2-}$ (1), $[Os_{10}C(CO)_{24}(\mu\text{-}I)]^-$ (2), $[Os_{10}C(CO)_{24}(\mu\text{-}I)_2]$ (3), and $[Os_{10}C(CO)_{23}\{P(OMe)_3\}(\mu\text{-}I)_2]$ (5)

the corresponding mono- and di-halogenated species respectively. The bromo-complexes were characterised on the basis of analytical and spectroscopic data (Table 2). The reaction with Cl_2 was carried out by the addition of a dilute solution of Cl_2 in dichloromethane to (1) dissolved in dichloromethane. Formation of the mono- and di-chloro-species can be monitored by i.r. spectroscopy. These complexes, however, could not be isolated in high yields because of a rapid additional reaction leading to the separation of a brown, insoluble precipitate. The formation of a similar brown compound was also observed in the reaction of I_2 and Br_2 with (1); the relative amount formed follows the order $Cl_2 > Br_2 > I_2$. In each case the yield of 'brown material' is sensitive to the duration and the temperature of the reaction; this product(s) could not be characterised by electron impact mass spectroscopy (e.i.m.s.) and microanalyses were inconclusive. On heating these species under reflux in acetone for an extended period of time (3 d) a faint brown solution which exhibits an i.r. spectrum characteristic of $[Os_{10}C(CO)_{24}(\mu\text{-}X)_2]$ (X = Cl, Br, or I) is obtained. This suggests that further halogenation or even polymerisation of $[Os_{10}C(CO)_{24}(\mu\text{-}X)_2]$ does not lead to breakdown of the Os_{10} skeleton. However, $[Os_{10}C(CO)_{24}(\mu\text{-}Br)_2]$ does undergo cluster fragmentation when treated with $CHBr_3$ at 80 °C to yield $[Os_2(CO)_6Br_4]$ as shown by e.i.m.s. and i.r. spectroscopy.

Reaction of $[Os_{10}C(CO)_{24}(\mu\text{-}I)_2]$ (3) *with some Nucleophiles in Polar Solvents.*—The neutral species (3) reacts rapidly with stoicheiometric amounts of iodide ion as $[NBu_4]I$ in solvents such as dichloromethane, acetone, or tetrahydrofuran at room temperature. The iodine atoms are sequentially lost from the cluster (3) to give firstly compound (2) and then (1) as shown in Figure 3. Iodine was detected by thin-layer chromatography (t.l.c.) and both (2) and (1) were identified by i.r. spectroscopy (Table 2). Sequential removal of I^+ also occurs when (3) is heated under reflux in CH_3CN over a period of 2 d, or when treated with L [L = $P(OMe)_3$, PPh_3, or pyridine (1:10)] in dichloromethane, acetone, or tetrahydrofuran at room temperature. The strength of the nucleophile and the polarity of the solvent appear to be the main factors that determine the rate of this reaction. Attempts to characterise the counter ions by ^1H n.m.r. spectroscopy were unsuccessful.

It would appear that the iodine atoms are removed by L as I^+ which is stabilised by two donor ligands as $[IL_2]^+$. Evidence for a cation of such stoicheiometry is the eventual formation of only $[Os_{10}C(CO)_{24}(\mu\text{-}I)]^-$ (2) in the reaction of $[Os_{10}C(CO)_{24}(\mu\text{-}I)_2]$ (3) with a two-fold excess of PPh_3. By monitoring this reaction using i.r. spectroscopy we have been able to show that $[Os_{10}C(CO)_{24}]^{2-}$ (1) is formed initially, leading us to suggest that the equilibrium (ii) is involved.

The reaction of (3) with CO (57.5 atm, 175 °C) in dichloro-

$$[Os_{10}C(CO)_{24}(\mu\text{-}I)_2] + [Os_{10}C(CO)_{24}]^{2-} \rightleftharpoons 2[Os_{10}C(CO)_{24}(\mu\text{-}I)]^- \quad \text{(ii)}$$

methane follows a similar course, where the incoming nucleophile displaces I$^+$. However, the nature of the counter ion is unknown. Analysis of the i.r. spectrum of the final product mixture* shows that in addition to the ν(CO) bands characteristic of (**2**), there are features present at 2 119 (sh), 2 113m, 2 078 (sh), and 2 071s cm^{-1} which could not be attributed to any known species. Purification of this mixture by t.l.c. using acetone–hexane (1:1) as eluant gave only (**2**) and (**1**) but a baseline was present that could not be extracted from the silica. Thus, the counter ion could well be some osmium carbonyl halogen species resulting from break-up of (**3**) that could have decomposed on the t.l.c. plates.

Treatment of osmium halogeno-clusters obtained from similar reactions to that of $[Os_{10}C(CO)_{24}]^{2-}$ with nucleophiles does not always lead to the removal of I$^+$. For example, the terminal iodide atom in $[Os_5(CO)_{15}I]^-$ seems to bear a negative charge rather than a positive as it is abstracted by Ag$^+$.[8] Furthermore, $[Os_4H_3(CO)_{12}(\mu\text{-}I)]$ which contains a similar iodine-bridged butterfly geometry to that found for (**2**) and (**3**), does not lose the μ-I ligand upon reaction with nucleophiles. In this case the cluster is deprotonated by excess L [L = I$^-$ or P(OMe)$_3$ in acetone] to give $[Os_4H_2(CO)_{12}(\mu\text{-}I)]^-$.[9] Nevertheless, the behaviour of the halogen derivatives of (**1**) under the conditions described above seems to be a characteristic for high nuclearity halogen osmium clusters. Indeed a similar reaction is shown by $[Os_8H(CO)_{22}(\mu\text{-}I)]$ obtained upon treatment of $[Os_8H(CO)_{22}]^-$ [7d] with I$^+$. In spite of the rearrangement of the Os$_8$ metal core during this reaction, addition of iodide ion reforms the monoanion with elimination of the bridging iodine atom.

Reaction of $[Os_{10}C(CO)_{24}(\mu\text{-}I)_2]$ (**3**) *with the Nucleophilic Reagent* $[N(PPh_3)_2][NO_2]$ *in Dichloromethane.*—The di-iodide (**3**) reacts with one equivalent of $[N(PPh_3)_2][NO_2]$ in dichloromethane at room temperature to give three products which were separated by t.l.c. using dichloromethane as eluant. The products, in order of increasing R_f, were compounds (**4**) (purple), (**4a**) (olive green), and (**4b**) (purple-red). The yield of (**4b**) was *ca.* twice that of (**4a**) and compound (**4**) was a minor product of the reaction. The i.r. spectra of these compounds (Table 2) suggest that (**4a**) and (**4b**) are monoanions (with very similar spectra), while (**4**) is a dianion. Attempted crystallisations of (**4a**) and (**4b**) from dichloromethane–isopropyl alcohol solution lead in each case to formation of (**4**), after several days at room temperature.

The dianion (**4**) is obtained in higher yield when a large excess of $[N(PPh_3)_2][NO_2]$ is used in the reaction. Compound (**4**) was initially characterised by analytical and spectroscopic data (Table 2); the i.r. spectrum exhibited a weak absorption at 1 724 cm^{-1} consistent with the presence of a terminal NO ligand. Crystals of $[N(PPh_3)_2]_2[Os_{10}C(CO)_{22}(NO)I]$ (**4**) were grown at 25 °C from dichloromethane–isopropyl alcohol by slow evaporation. An *X*-ray structure analysis confirmed the presence of a terminal nitrosyl ligand, although the NO group could not be distinguished from the CO groups. The dianion is disordered in the crystal (see Experimental section) and the structure of one component of the disorder is illustrated in Figure 4; selected bond lengths and angles are given in Table 4. In the dianion there is a terminal iodine ligand bonded to a capping Os atom with a bond distance [mean Os–I 2.756(10) Å] slightly longer than the mean bridging Os–I bond lengths of 2.723(4) in (**2**), 2.736(5) in (**3**), and 2.733(3) Å in $[Os_{10}C(CO)_{23}\{P(OMe)_3\}(\mu\text{-}I)_2]$ (**5**). In general bridging bond lengths are longer than terminal, so it seems probable that this apparent lengthening of the Os–I terminal bond in (**4**) is caused by the nature of the disorder of the dianion in the crystal (see Experimental section). Unlike the cluster species with 'opened caps' (**2**), (**3**), and (**5**), in the tetracapped octahedral structure of (**4**) the mean Os–Os bond lengths for the central Os$_6$ core and for the capping tetrahedra, 2.884(3) and 2.788(3) Å, are very similar to the equivalent mean distances in the dianion $[Os_{10}C(CO)_{24}]^{2-}$ (**1**), 2.883(1) and 2.786(1) Å respectively.[3] The overall distributions of the surface ligands in the two dianions (**1**) and (**4**) are very similar and it is interesting that their $[N(PPh_3)_2]^+$ salts and that of the interstitial tetrahydrido-dianion $[Os_{10}H_4(CO)_{24}]^{2-}$ are isomorphous.[10]

Table 4. Selected bond lengths (Å) and angles (°) for $[Os_{10}C(CO)_{22}(NO)I]^{2-}$ (**4**)*

(*i*) Bond lengths

Os–Os within octahedron

Os(2)–Os(3)	2.888(3)	Os(2)–Os(4)	2.880(3)
Os(2)–Os(6)	2.879(4)	Os(2)–Os(10)	2.869(4)
Os(3)–Os(4)	2.864(3)	Os(3)–Os(6)	2.889(3)
Os(3)–Os(8)	2.879(4)	Os(4)–Os(8)	2.871(4)
Os(4)–Os(10)	2.907(3)	Os(6)–Os(8)	2.900(3)
Os(6)–Os(10)	2.875(3)	Os(8)–Os(10)	2.902(3)

Mean 2.884(3)

Os–Os involving capping atoms

Os(1)–Os(2)	2.786(3)	Os(1)–Os(3)	2.815(3)
Os(1)–Os(4)	2.780(4)	Os(5)–Os(2)	2.790(3)
Os(5)–Os(6)	2.801(3)	Os(5)–Os(10)	2.770(3)
Os(7)–Os(3)	2.775(3)	Os(7)–Os(6)	2.785(3)
Os(7)–Os(8)	2.779(3)	Os(9)–Os(4)	2.779(4)
Os(9)–Os(8)	2.816(3)	Os(9)–Os(10)	2.776(3)

Mean 2.788(3)

Os–iodine*

Os(5)–I(2)	2.761(10)	Os(7)–I(1)	2.751(10)

Mean 2.756(10)

Os–carbido C

Range	1.96(4)—2.13(4)	Mean	2.04(4)

Os–carbonyl C

Range	1.74(7)—1.98(7)	Mean	1.77(7)

Carbonyl C–O

Range	1.05(8)—1.30(8)	Mean	1.18(8)

(*ii*) Bond angles

I(2)–Os(5)–Os(2)	107.0(2)	I(1)–Os(7)–Os(6)	101.9(2)
I(2)–Os(5)–Os(6)	104.7(2)	I(1)–Os(7)–Os(8)	99.6(2)
I(2)–Os(5)–Os(10)	165.4(2)	I(1)–Os(7)–Os(3)	159.8(2)

Os–C–O (carbonyl)

Range	158(5)—177(5)	Mean	170(5)

* There is a 50:50 disorder of the dianion (**4**) giving two iodine sites of equal occupancy; the NO ligand could not be distinguished from the CO ligands.

Work by Gladfelter and co-workers[11] has established the general pattern of reactions of neutral carbonyl clusters with $[N(PPh_3)_2][NO_2]$, which as shown by equation (iii) (L = CO,

---

* ν(CO)/cm^{-1}: 2 119 (sh), 2 113m, 2 091m, 2 078 (sh), 2 071s, 2 062 (sh), 2 057vs, 2 022vs, 2 019s; compare to spectra of (**1**), (**2**), and (**3**) in Table 2.

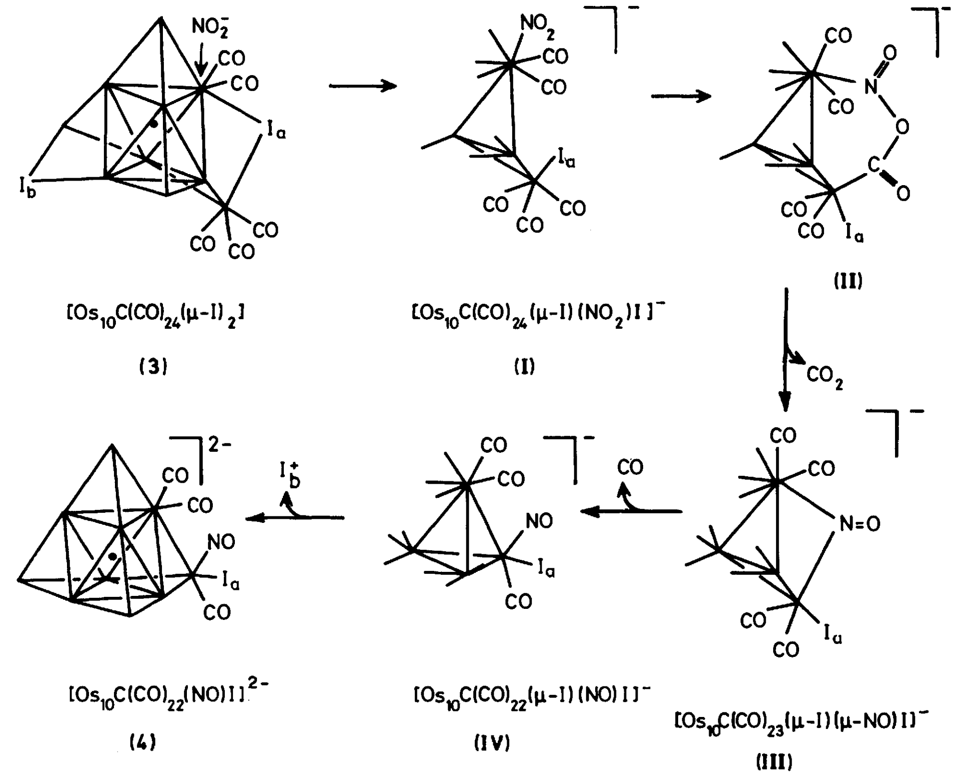

Scheme 1. Suggested mechanism for the formation of $[Os_{10}C(CO)_{22}(NO)I]^{2-}$ (4)

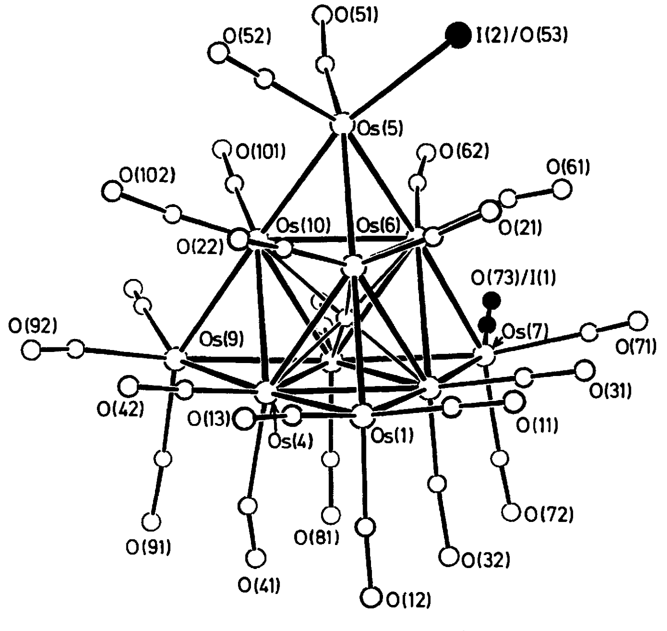

Figure 4. Structure of $[Os_{10}C(CO)_{22}(NO)I]^{2-}$ (4). Only one component of the disorder is shown. It was not possible to differentiate between the terminal NO and CO ligands (see Figure 1 for numbering scheme)

$$[M(CO)(CO)_mL_n] + [N(PPh_3)_2][NO_2] \longrightarrow [N(PPh_3)_2][M(NO)(CO)_mL_{n-1}] + CO_2 + L \quad (iii)$$

PR_3, or other two-electron donors) result in the substitution of two two-electron donors by a linear nitrosyl three-electron donor and a negative charge. These reactions have generally been shown to have a high degree of specificity, with only one product being detected. On the basis of kinetic and chemical data possible mechanisms involving initial attack of $[NO_2]^-$ on co-ordinated CO have been proposed.[11]

A different mechanism is required for the reaction of halogen-containing clusters with $[NO_2]^-$ because the electronegative character of the halogen ligand results in a positive polarisation of the metal to which it is attached, making it the most probable site for nucleophilic attack. The ability of the halogen to bond either in a terminal (one-electron donor) or a bridging (three-electron donor) fashion and its potential for interchange between these two modes will also influence the course of the reaction and the product distribution. In the reaction of the iodo-derivative (**3**) with $[N(PPh_3)_2][NO_2]$ the product (**4**) has a terminal iodine attached to a capping Os atom, indicating that initial attack is at an osmium atom of the central octahedron. A reasonable mechanism for the subsequent stages, which involves reaction of a co-ordinated nitrito-ligand with a carbonyl followed by loss of CO_2 to give a nitroso-bridged species (**III**), is shown in Scheme 1. The dissociation of the second bridging iodine atom 'I_b' must occur at some stage after the formation of the initial intermediate (**I**), because reaction of the monoiodide $[Os_{10}C(CO)_{24}(\mu\text{-}I)]^-$ (**2**) with excess $[NO_2]^-$ does not give (**4**), the dianion $[Os_{10}C(CO)_{24}]^{2-}$ (**1**) being the only product. The unidentified monoanions (**4a**) and (**4b**), isolated from the reaction of (**3**) when only one equivalent of $[NO_2]^-$ was used, may correspond to two of the intermediates shown in Scheme 1, or they may be isomers of the same species.

Reaction of $[Os_{10}C(CO)_{24}(\mu\text{-}I)_2]$ (**3**) *with* $P(OMe)_3$ *in Non-polar Solvents.*—The reaction of the di-iodide (**3**) with $[NO_2]^-$ strongly suggested that activation of this cluster could occur through an opening up of the μ-I bridges. Although such a process was not implicated in the reactions of (**3**) with other nucleophiles (PPh_3, pyridine, or CO) under similar conditions,

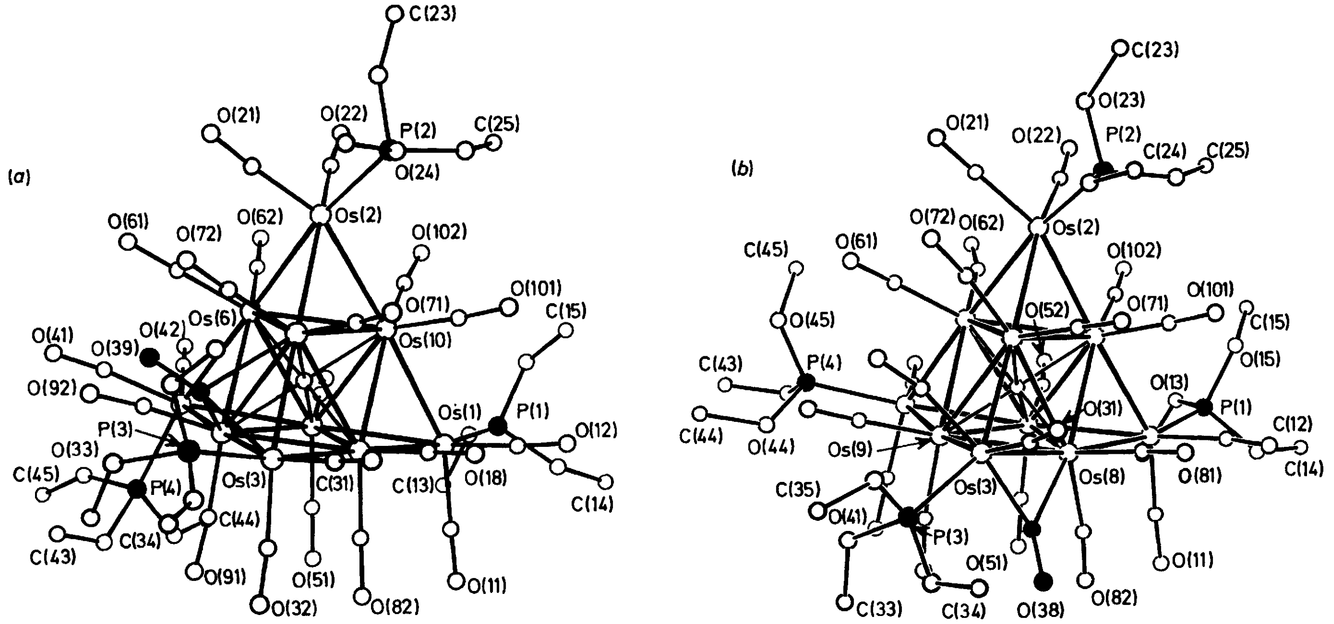

Figure 5. Structures of the two isomers of $[Os_{10}C(CO)_{21}\{P(OMe)_3\}_4]$. (*a*) Isomer (**6**), from the reaction of $P(OMe)_3$ with (**3**), showing a μ_3 bridging carbonyl ligand; this isomer has an approximately collinear arrangement of two P–Os–Os–Os–P units along two edges of the giant tetrahedron. (*b*) Isomer (**6a**), from the reaction of $P(OMe)_3$ with $[Os_{10}H_2C(CO)_{24}]$, showing a μ bridging carbonyl; no two phosphites approximate to linearity with any edge of the Os_{10} core [See Figure 1 for numbering scheme and Experimental section for discussion of the disorder in (**6**), which has crystallographic $\bar{4}$-fold symmetry]

the reaction of (**3**) with $P(OMe)_3$ was investigated under conditions that would not favour dissociation of I^+, *i.e.* by using non-polar solvents * for the reaction.

Compound $[Os_{10}C(CO)_{24}(\mu\text{-}I)_2]$ (**3**) does not react with excess $P(OMe)_3$ when heated in refluxing toluene (b.p. 100.6 °C) for prolonged periods. In refluxing xylene (b.p. 139.1 °C), however, reaction does occur and is complete after 3.5 h. A mixture of products which can be extracted with dichloromethane was obtained and purified by t.l.c. techniques. From the complex product mixture six complexes (**5**)—(**10**) were separated in sufficient yields to be characterised by i.r. spectroscopy in the ν(CO) region (Table 2), however no e.i.m.s. spectra could be obtained on any of these products. Compounds (**5**), (**6**), and (**8**) were the major products of the reaction.

Microanalytical and spectroscopic data, together with an *X*-ray analysis, have shown the neutral species (**6**) to be $[Os_{10}C(CO)_{21}\{P(OMe)_3\}_4]$. A compound of this formulation, (**6a**), which was also characterised by an *X*-ray analysis, was previously obtained (in these laboratories) in low yield from the reaction of $[Os_{10}H_2C(CO)_{24}]$ with $P(OMe)_3$ in refluxing xylene, probably according to equation (iv).

$$[Os_{10}H_2C(CO)_{24}] + 4P(OMe)_3 \longrightarrow [Os_{10}C(CO)_{21}\{P(OMe)_3\}_4] + \text{‘}H_2\text{’} + 3CO \quad \text{(iv)}$$

The results of *X*-ray structure determinations for both (**6**) and (**6a**) are given here for comparison. The molecular structure of the two isomers are shown in Figure 5(*a*) and (*b*) respectively, and selected bond lengths and angles are given in Table 5. The *X*-ray analysis establishes that (**6**) and (**6a**) both have structures with the four phosphite ligands distributed one on each of the four capping Os atoms of the tetracapped octahedral Os_{10} core. In both clusters three of the original $Os(CO)_3$ capping groups present in the respective starting materials have had one CO ligand replaced by a phosphite ligand, and the fourth $P(OMe)_3$ group in both has added to the fourth capping osmium atom, Os(3), without loss of CO. It is well established that the 24 carbonyl ligands on the surface of $[Os_{10}C(CO)_{24}]^{2-}$ are very closely packed,[3] and that in the hydrido-derivative higher surface ligand density is avoided by the H atom adopting an interstitial location.[4] In each of the molecules (**6**) and (**6a**) the addition of a 25th ligand at Os(3) causes considerable ligand overcrowding in this region resulting in one of the CO ligands attached to Os(3), in both molecules, adopting a bridging mode which is rare in osmium cluster compounds. In isomer (**6**) this gives a μ_3-CO ligand and in (**6a**) the bridging carbonyl adopts a μ_2 bonding mode. The main difference between the two isomers is seen in the positioning of the phosphite ligands. It can be seen in Figure 5(*a*) that in isomer (**6**) there are two approximately collinear P–Os–Os–Os–P units, along two of the edges of the giant Os_{10} tetrahedron, related by a C_2 axis; in contrast Figure 5(*b*) shows that in isomer (**6a**) no two phosphite ligands approximate to collinearity with the same edge of the Os_{10} core. The mean Os–Os distance in the octahedral core of (**6a**) [2.898(2) Å] is slightly longer than that in (**6**) [2.882(2) Å] which is close to the analogous value for the other clusters with closed capping groups, (**1**) and (**4**). The mean Os–Os distance in the capping groups of (**6a**) [2.833(2) Å] is also significantly longer than that of 2.818(2) Å in (**6**), and considerably longer than the corresponding mean values of 2.786(1) Å in (**1**)[3] and 2.788(3) Å in (**4**). It seems possible that this slight expansion of the metal core has resulted from the attempt to accommodate the extra surface ligand in (**6a**); that this effect is not noticed in (**6**) may be a consequence of the disorder of the molecule in the crystal (see Experimental section).

A combination of spectroscopic and analytical data together with an *X*-ray structure determination established that (**5**) is the neutral compound $[Os_{10}C(CO)_{23}\{P(OMe)_3\}(\mu\text{-}I)_2]$, but the other products (**7**)—(**10**) have not been fully characterised (see Table 2). The structure of (**5**) is shown in Figure 6 and selected bond lengths and angles are given in Table 3 for comparison

---

* Non-polar solvents were initially avoided due to the lack of solubility of compound (**3**) in such solvents at room temperature.

Table 5. Selected bond lengths (Å) and angles (°) for the two isomers of $[Os_{10}C(CO)_{21}\{P(OMe)_3\}_4]$, **(6)** and **(6a)**

	(6) *	**(6a)**
(*i*) Bond lengths		
Os–Os within octahedron		
5–6	2.875	2.888(1)
5–8	2.875	2.898(2)
5–9	2.896(3)	2.884(2)
5–10	8.896	2.838(2)
6–7	2.875	2.886(2)
6–9	2.875	2.879(2)
6–10	2.875	2.917(2)
7–8	2.875	2.926(1)
7–9	2.896	3.051(2)
7–10	2.896	2.832(2)
8–9	2.875(2)	2.883(2)
8–10	2.875	2.896(2)
Mean	2.882(2)	2.898(2)
Os–Os involving capping atoms		
1–5	2.836	2.749(2)
1–8	2.781	3.016(2)
1–10	2.836	2.764(1)
2–6	2.781	2.800(2)
2–7	2.836	2.941(2)
2–10	2.836	2.771(1)
3–7	2.836	2.814(2)
3–8	2.781(2)	2.813(2)
3–9	2.836(2)	2.848(2)
4–5	2.836	2.838(2)
4–6	2.781	2.775(2)
4–9	2.836	2.863(2)
Mean	2.818(2)	2.833(2)
Os–P		
Os(1)–P(1)	2.254	2.238(10)
Os(2)–P(2)	2.254	2.275(9)
Os(3)–P(3)	2.254(14)	2.310(11)
Os(4)–P(4)	2.254	2.269(10)
Mean	2.254(14)	2.298(10)
Os–carbido C		
Range	2.02(3)—2.05(3)	2.00(2)—2.08(2)
Mean	2.04(3)	2.05(2)
Os–carbonyl C (terminal)		
Range	1.77(3)—1.80(3)	1.81(4)—1.94(4)
Mean	1.79(3)	1.86(4)
Os–bridging carbonyl C		
Os(3)–C(38)[C(39)]	2.007(20)	1.99(5)
Os(7)–C(39)	2.402(20)	
Os(8)–C(38)		2.47(6)
Os(9)–C(39)	2.402(20)	
P–O		
Range	1.54(3)—1.57(3)	1.53(3)—1.65(3)
Mean	1.56(3)	1.58(3)
(*ii*) Bond angles		
P–Os–Os		
P(3)–Os(3)–Os(7)	110.0(4)	150.0(2)
P(3)–Os(3)–Os(8)	169.9(4)	141.3(2)
P(3)–Os(3)–Os(9)	110.1(3)	106.8(3)
P(3)–Os(3)–C(39)[C(38)]	63.6(8)	87(2)
P(1)–Os(1)–Os(5)		115.7(3)
P(1)–Os(1)–Os(8)		169.7(2)
P(1)–Os(1)–Os(10)		109.8(2)
P(2)–Os(2)–Os(6)		163.6(2)
P(2)–Os(2)–Os(7)		103.5(2)
P(2)–Os(2)–Os(10)		108.0(2)
P(4)–Os(4)–Os(5)		169.0(2)
P(4)–Os(4)–Os(6)		109.5(2)
P(4)–Os(4)–Os(9)		109.6(3)

Angles at bridging carbonyl

Os(3)–C(39)–Os(7)	79.5(6)	Os(3)–C(38)–Os(8)	77(2)
Os(3)–C(39)–Os(9)	79.5(6)	Os(3)–C(38)–O(38)	157(5)
Os(3)–C(39)–O(39)	162(7)	Os(8)–C(38)–O(38)	126(4)
Os(7)–C(39)–Os(9)	74.1(7)		
Os(7)–C(39)–O(39)	115(5)		
Os(9)–C(39)–O(39)	115(5)		

* For ease of comparison with **(6a)** a full numbering scheme for **(6)** is shown in Figure 5(*a*) and all the bond lengths are given here; the e.s.d.s for the crystallographically unique lengths are given in parentheses.

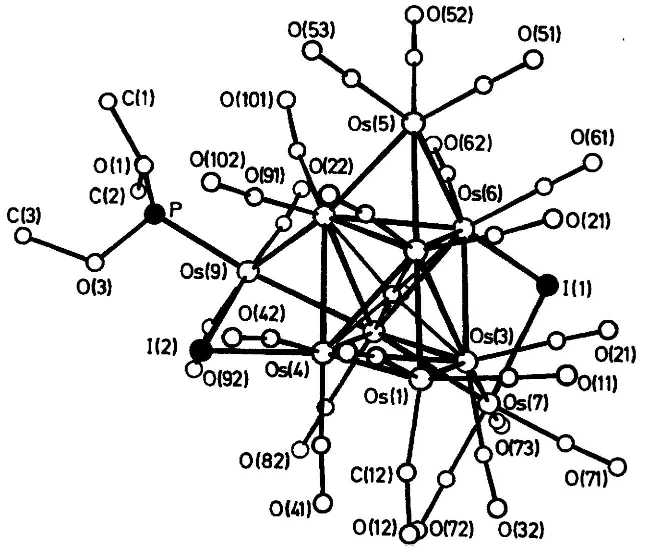

Figure 6. Structure of $[Os_{10}C(CO)_{23}\{P(OMe)_3\}(\mu\text{-}I)_2]$ **(5)** (see Figure 1 for numbering scheme)

with the other iodo-bridged species **(2)** and **(3)**. Figure 3 shows that these species have core geometries related to that of **(1)** by the opening of capping tetrahedral groups by the μ-I ligands. The structure of **(5)** is similar to that of **(3)** with the phosphite ligand replacing a carbonyl on the Os atom of an 'open cap', Os(9) (Figure 6). The two bonds to the central octahedral core from the 'open-cap' $Os(CO)_2\{P(OMe)_3\}$ group [Os(9)–Os(8) 2.897(2) and Os(9)–Os(10) 2.851(2) Å] are significantly longer than the bonds from the corresponding $Os(CO)_3$ group [Os(7)–Os(3) 2.825(2) and Os(7)–Os(8) 2.817(2) Å], and are also longer than the analogous bonds in the non-phosphito-compounds **(3)** [mean 2.829(4) Å] and **(2)** [mean 2.840(2) Å]. In **(5)** the bridged 'wing-tip' distance from the $Os(CO)_2\{P(OMe)_3\}$ group [Os(9) ··· Os(4) 3.933(2) Å] is considerably longer than the second iodo-bridged 'wing-tip' distance [Os(7) ··· Os(6) 3.878(2) Å]. These may be compared with the analogous Os ··· Os distances of 3.907(2) Å in **(2)** and of 3.893(4) Å (mean) in (3). The central octahedral core in these iodo-bridged species have mean Os–Os bond lengths of 2.901(2) for (2), 2.911(4) for (3), and 2.910(2) Å for (5) which are all slightly longer than that in the unsubstituted dianion (1) [2.883(1) Å]. The mean distances from the tetrahedrally capping Os atoms to the central octahedron are very similar in all four species, 2.792(2) for (2), 2.790(4) for (3), 2.784(2) for (5), and 2.786(1) Å for the dianion (1).[3]

As anticipated, the neutral species $[Os_{10}C(CO)_{23}\{P(OMe)_3\}(\mu\text{-}I)_2]$ (5) reacts with excess iodide ion as $[NBu_4]I$ in acetone in a similar fashion to that found for (3). The sequential formation of a monoanion and a dianion is observed when the reaction is monitored by i.r. spectroscopy [see Table 2 for the i.r. spectra of the monoanion (5a) and dianion (5b)]. The neutral species is reformed on addition of excess I_2 to a solution of monoanion (5a) or the dianion (5b) in dichloromethane. These reactions are summarised in equation (v).

$$\underset{(5)}{[Os_{10}C(CO)_{23}\{P(OMe)_3\}(\mu\text{-}I)_2]} \underset{I_2}{\overset{I^-}{\rightleftharpoons}} \underset{(5a)}{[Os_{10}C(CO)_{23}\{P(OMe)_3\}(\mu\text{-}I)]^-}$$

$$I_2 \uparrow\downarrow I^-$$

$$\underset{(5b)}{[Os_{10}C(CO)_{23}\{P(OMe)_3\}]^{2-}} \quad \text{(v)}$$

Attempts to obtain X-ray quality crystals of compound (8) have failed to date. Microanalytical data are inconclusive and the degree of replacement of CO by $P(OMe)_3$ is unknown. As (8) reacts with excess iodide ion in acetone to give only a mono-anionic cluster (8a) as shown by i.r. spectroscopy (Table 2) it is presumed that (8) contains only one μ-I ligand. The anion (8a) behaves similarly to the systems discussed above on reaction with iodine, and regenerates the neutral complex (8).

As a consequence of the number of products derived from the reaction of $[Os_{10}C(CO)_{24}(\mu\text{-}I)_2]$ (3) with $P(OMe)_3$, a discussion of the mechanism of this reaction must be speculative. Bearing in mind the views expressed above about activation by halogens, it seems reasonable to propose that formation of (5) may involve the initial creation of an additional co-ordination site for the $P(OMe)_3$ ligand *via* opening of an iodo-bridge. Ejection of a CO ligand followed by reformation of the μ-I bridge would give compound (5) as illustrated in Scheme 2. In the case of compound (6), with the addition of four $P(OMe)_3$ ligands and loss of I_2, it is not possible at this stage of our investigations to indicate the possible sequence of the process involved in the formation of this compound.

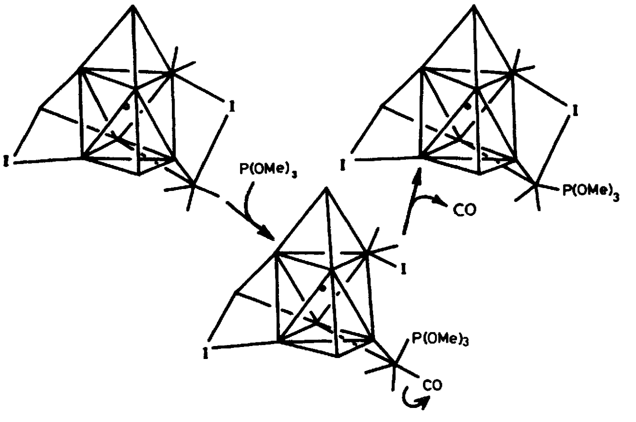

Scheme 2. Suggested mechanism for the formation of $[Os_{10}C(CO)_{23}\{P(OMe)_3\}(\mu\text{-}I)_2]$ (5)

Conclusions

In this work we have shown that the interaction of $[Os_{10}C(CO)_{24}]^{2-}$ with the electrophile 'I^+' (I_2) leads to species which show enhanced reactivity towards nucleophilic attack. This tends to support the view that the ability of the μ-I ligand to interchange with a terminal bonding state may have the effect of generating a vacant co-ordination site in the molecule for the approach of an incoming substrate. These results agree with our previous suggestions and findings.

Experimental

All reactions were carried out under nitrogen using dry degassed solvents. Autoclave reactions were carried out in a Roth Laboratory autoclave of 100-cm^3 capacity. Infrared spectra were recorded as solutions in 0.5-mm CaF_2 cells on a Perkin-Elmer 257 spectrometer using carbon monoxide as calibrant. Thin-layer chromatography plates were obtained from Merck and consisted of glass plates (20 × 20 cm) coated with a 0.25-mm layer of silica gel.

Preparation of $[Os_{10}C(CO)_{24}(\mu\text{-}I)_2]$ (3).—The salt $[N(PPh_3)_2]_2[Os_{10}C(CO)_{24}]$ (1) (570 mg, 0.165 mmol) was dissolved in CH_2Cl_2 (125 cm^3) and stirred with I_2 (190 mg, 0.75 mmol, 4.8 mol equiv.) for 1 h during which time the colour of the solution changed from dark red to brown. The solvent and excess iodine were first removed on a rotary evaporator, the product was separated from a small amount of dark insoluble material by extraction into CH_2Cl_2 at room temperature and then finally recrystallised from CH_2Cl_2–MeOH by slow evaporation (yield 363 mg, 82.1%). The dark brown crystals of (3) were characterised by i.r. spectroscopy (Table 2), microanalysis (Found: C, 11.1; I, 8.2. Calc. for $C_{25}I_2O_{24}Os_{10}$: C, 10.6; I, 8.9%), and X-ray structure analysis.

Preparation of $[N(PPh_3)_2][Os_{10}C(CO)_{24}(\mu\text{-}I)]$ (2).—The dark red salt of (1) (50 mg, 0.014 mmol) in CH_2Cl_2 (13 cm^3) was stirred with 2.4 mol equiv. of I_2 (8.3 mg, 0.033 mmol) for 10 min at room temperature to give a red-purple solution. MeOH (10 cm^3) was then added and most of the CH_2Cl_2 removed prior to crystallisation by slow evaporation. The red-purple crystals of (2) (yield 31 mg, 70.7%) were characterised by i.r. spectroscopy (Table 2), microanalysis (Found: C, 22.7; H, 0.80. Calc. for $C_{61}H_{30}INO_{24}Os_{10}P_2$: C, 22.5; H, 0.90%), and X-ray structure analysis.

Preparation of $[Os_{10}C(CO)_{24}(\mu\text{-}Br)_2]$.—To the salt (1) (50 mg, 0.014 mmol) dissolved in CH_2Cl_2 (10 cm^3) was added dropwise a fresh solution of Br_2 in CH_2Cl_2 (8.7 mg, 0.054 mmol, 3 cm^3). The reaction mixture was stirred at room temperature for 15 min. The solution was concentrated and the mixture separated by t.l.c. using acetone–hexane (1:4) as eluant to give as the band of highest R_f, $[Os_{10}C(CO)_{24}(\mu\text{-}Br)_2]$. A small amount of the monoanion $[Os_{10}C(CO)_{24}(\mu\text{-}Br)]^-$, characterised by i.r. spectroscopy, and an insoluble dark brown material were the other products of the reaction. Crystals of $[Os_{10}C(CO)_{24}(\mu\text{-}Br)_2]$ were obtained from CH_2Cl_2–MeOH by slow evaporation and were characterised by i.r. spectroscopy (Table 2), yield 15 mg, 41.7%.

Preparation of $[N(PPh_3)_2][Os_{10}C(CO)_{24}(\mu\text{-}Br)]$.—To the salt (1) (20 mg, 0.005 mmol), dissolved in CH_2Cl_2 (10 cm^3) was added dropwise a fresh solution of Br_2 in CH_2Cl_2 (1.7 mg, 0.011 mmol, 1.5 cm^3). The mixture was stirred for 5 min at room

Table 6. Crystal and *X*-ray structure analysis data[a]

	(2)	**(3)**[b]	**(4)**[c]	**(5)**[d]	**(6)**[e]	**(6a)**
Molecular formula	$C_{61}H_{30}INO_{24}Os_{10}P_2$	$C_{25}I_2O_{24}Os_{10}$	$C_{95}H_{60}IN_3O_{23}Os_{10}P_4$	$C_{28}H_{11}Cl_2I_2O_{26}Os_{10}P$	$C_{34}H_{36}O_{33}Os_{10}P_4$	
M	3 251.75	2 840.06	3 764.33	3 021.1	2 998.5	
Crystal dimensions (mm)	0.16 × 0.12 × 0.10	0.25 × 0.23 × 0.08	0.23 × 0.18 × 0.11	0.19 × 0.16 × 0.12	0.35 × 0.19 × 0.08	0.20 × 0.12 × 0.04
Space group	$P\bar{1}$	$P2_12_12_1$	$P\bar{1}$	$P2_1/n$	$P4_2/nmc$	$P\bar{1}$
a/Å	19.161(3)	30.676(4)	27.366(3)	23.887(3)	16.222(3)	20.600(2)
b/Å	19.086(3)	12.323(2)	17.569(3)	19.135(3)	16.222(3)	12.782(2)
c/Å	10.446(2)	11.700(2)	10.459(2)	11.106(2)	10.988(3)	11.303(2)
α/°	91.12(2)	90	96.57(2)	90	90	92.36(2)
β/°	84.07(2)	90	100.39(3)	100.74(2)	90	102.57(2)
γ/°	109.60(3)	90	85.74(2)	90	90	90.11(2)
U/Å^3	3 579.2	4 422.84	4 906.35	4 987.4	2 891.5	2 902.15
D_c/g cm^{-3}	3.02	4.26	2.55	4.02	3.44	3.43
Z	2	4	2	4	2	2
F(000)	2 876	4 808	3 548	5 208	2 648	2 648
μ(Mo-K_α)/cm^{-1}	174.95	288.82	130.98	257.5	212.1	212.1
No. unique observed data [$I/\sigma(I) \geq 3.0$]	7 936	2 406	3 308	4 134	651	4 819
No. azimuthal scan data	422	372	283	331	271	224
Relative transmission factors						
min.	0.639	0.646	0.679	0.438	0.550	0.304
max.	1.00	1.00	1.00	1.00	1.00	1.00
Anisotropic atom	I,Os,P	I,Os	I,Os,P	I,Os,P	Os,P	Os,P
R	0.094	0.058	0.054	0.059	0.061	0.053
$R'(=\Sigma w^{\frac{1}{2}}\Delta/\Sigma w^{\frac{1}{2}}\|F_o\|)$	0.095	0.056	0.053	0.056	0.067	0.052

[a] Details pertaining to all structures: D_m, not measured; Mo-K_α radiation, λ = 0.710 69 Å; 2θ range, 3—25°; scan mode, ω–2θ; method of Os atom location, Patterson; method of light-atom location, Fourier difference; refinement technique, blocked full-matrix least squares; weighting scheme, $w = [\sigma^2(F_o)]^{-1}$; empirical absorption corrections.[12] [b] Refinement in the opposite 'hand' to the co-ordinates given gave *R* and *R*′ values of 0.063 and 0.062 respectively. [c] There is a 50:50 disorder of the cluster dianion (see Experimental section). [d] The CH_2Cl_2 molecule is disordered. [e] The cluster molecule is disordered (see Experimental section).

temperature. The solution was concentrated and the mixture separated by t.l.c. using acetone–hexane (1:4) as eluant to give as the band of second highest R_f $[N(PPh_3)_2][Os_{10}C(CO)_{24}(\mu\text{-Br})]$, the major product of the reaction, and traces of $[Os_{10}C(CO)_{24}]^{2-}$. Crystals were obtained from CH_2Cl_2–MeOH and were characterised by i.r. spectroscopy (Table 2).

Reaction of $[N(PPh_3)_2]_2[Os_{10}C(CO)_{24}]$ (**1**) *with* Cl_2.—A solution of Cl_2 in CH_2Cl_2 was added dropwise to a solution of (**1**) dissolved in CH_2Cl_2 (20 mg, 0.005 mmol, in 5 cm^3). A dark solid precipitated which was insoluble in MeCN, MeOH, $CHCl_3$, CH_2Cl_2 or hexane but dissociated to give $[Os_{10}C(CO)_{24}(\mu\text{-Cl})_2]$ after reflux in acetone for 3 d. The CH_2Cl_2 soluble fraction was chromatographed on silica plates using acetone–hexane (1:2) as eluant to give $[Os_{10}C(CO)_{24}(\mu\text{-Cl})_2]$ as the fastest moving band (yield 10.6 mg, 30%) and $[N(PPh_3)_2][Os_{10}C(CO)_{24}(\mu\text{-Cl})]$ as the second band (yield 8.9 mg, 51.6%).

Reaction of $[N(PPh_3)_2]_2[Os_{10}C(CO)_{24}]$ (**1**) *with* $CHBr_3$.—A solution of compound (**1**) (20 mg, 0.005 mmol) in $CHBr_3$ (8 cm^3) was heated to 80 °C. After a few minutes a drastic colour change from dark brown to pale yellow was observed. The mixture was cooled to 4 °C for 12 h and the pale yellow solid which precipitated was filtered off and washed with cold $CHBr_3$. It was shown to be $[Os_2(CO)_6Br_4]$ by i.r. and mass spectroscopy (Found: C, 8.40. Calc. for $C_6Br_4O_6Os_2$: C, 8.30%): highest peak M^+, 868; *m/e* $\{[Os_2(CO)_6Br_4]^+\}$; ν(CO)(acetone) 2 132w (sh), 2 050s, br, and 1 960w cm^{-1}.

Stability of $[Os_{10}C(CO)_{24}(\mu\text{-I})_2]$ (**3**) *and* $[Os_{10}C(CO)_{24}(\mu\text{-I})]^-$ (**2**) *in Various Solvents*.—Each of the compounds (**2**) and (**3**) was heated in turn under reflux in CH_2Cl_2, MeOH, acetone, Pr^{i}OH, and hexane for 3 d during which time no change was observed in the respective i.r. spectra. However when MeCN was used as the solvent, dissociation of both compounds was observed to give $[Os_{10}C(CO)_{24}]^{2-}$ which was detected by i.r. spectroscopy.

Reaction of $[Os_{10}C(CO)_{24}(\mu\text{-I})_2]$ (**3**) *with Nucleophiles*, L.—(*a*) L = I^-, $P(OMe)_3$, PPh_3, *or pyridine*. The neutral species (**3**) (10 mg) and ligand L (10 mol equiv.) were stirred together in acetone, tetrahydrofuran, or CH_2Cl_2 (4 cm^3) at room temperature. Total conversion to $[Os_{10}C(CO)_{24}]^{2-}$ was observed *via* the monoanion $[Os_{10}C(CO)_{24}(\mu\text{-I})]^-$, in all solvents; in acetone conversion took place in less than 1 h for L = $P(OMe)_3$ and in 48 h for L = pyridine.

(*b*) L = PPh_3 (2 *mol equiv., in acetone*). The species (**3**) (10 mg) was stirred with 2 mol equiv. of PPh_3 (1.8 mg) in acetone (4 cm^3) at room temperature for 10 h. Total conversion to the monoanion $[Os_{10}C(CO)_{24}(\mu\text{-I})]^-$ was observed by i.r. spectroscopy.

(*c*) L = $[Os_{10}C(CO)_{24}]^{2-}$. When $[N(PPh_3)_2]_2[Os_{10}C(CO)_{24}]$ (12 mg) and $[Os_{10}C(CO)_{24}(\mu\text{-I})_2]$ (10 mg, 1 mol

Table 7. Fractional atomic co-ordinates for the anion in $[N(PPh_3)_2][Os_{10}C(CO)_{24}(\mu\text{-}I)]$ (**2**)

Atom	*x*	*y*	*z*	Atom	*x*	*y*	*z*
Os(1)	0.299 87(9)	−0.155 74(9)	−0.145 58(17)	C(51)	0.263 3(26)	−0.341 2(26)	0.352 7(48)
Os(2)	0.240 79(9)	−0.253 27(9)	0.064 28(16)	O(51)	0.317 7(21)	−0.328 0(21)	0.403 8(38)
Os(3)	0.220 10(9)	−0.111 34(8)	0.062 24(16)	C(52)	0.185 3(28)	−0.440 6(29)	0.180 5(53)
Os(4)	0.147 09(9)	−0.225 47(9)	−0.110 60(16)	O(52)	0.195 0(19)	−0.493 5(19)	0.132 1(35)
Os(5)	0.178 28(10)	−0.357 24(9)	0.261 36(17)	C(53)	0.114 1(26)	−0.413 5(26)	0.401 5(50)
Os(6)	0.153 33(10)	−0.218 07(9)	0.281 51(16)	O(53)	0.074 5(20)	−0.447 5(19)	0.476 0(36)
Os(7)	0.119 22(10)	−0.039 64(9)	0.167 19(17)	C(61)	0.233 3(24)	−0.198 4(23)	0.377 4(43)
Os(8)	0.054 88(9)	−0.190 55(9)	0.098 98(16)	O(61)	0.284 4(22)	−0.181 8(22)	0.437 0(42)
Os(9)	−0.004 22(9)	−0.304 18(9)	−0.076 41(17)	C(62)	0.086 0(24)	−0.269 3(24)	0.409 0(44)
Os(10)	0.084 45(9)	−0.328 87(9)	0.100 84(16)	O(62)	0.042 1(19)	−0.296 1(18)	0.488 7(35)
I	0.132 1(2)	−0.097 1(1)	0.397 3(2)	C(71)	0.190 4(28)	0.040 5(28)	0.183 1(52)
C	0.148 5(18)	−0.219 0(18)	0.084 1(33)	O(71)	0.245 7(18)	0.096 8(18)	0.219 6(33)
C(11)	0.387 8(32)	−0.112 3(31)	−0.102 5(29)	C(72)	0.038 3(23)	−0.011 3(23)	0.247 5(42)
O(11)	0.444 5(20)	−0.077 6(20)	−0.055 0(37)	O(72)	−0.001 7(21)	0.013 2(21)	0.313 0(37)
C(12)	0.328 4(23)	−0.219 0(23)	−0.259 0(42)	C(73)	0.107 9(25)	−0.007 1(25)	0.008 8(47)
O(12)	0.353 3(19)	−0.255 1(19)	−0.328 3(36)	O(73)	0.102 0(19)	0.019 3(20)	−0.100 9(37)
C(13)	0.309 5(21)	−0.089 0(21)	−0.273 5(40)	C(81)	0.002 8(24)	−0.147 6(24)	−0.004 3(45)
O(13)	0.315 5(20)	−0.048 1(20)	−0.368 1(37)	O(81)	−0.033 4(18)	−0.125 6(18)	−0.064 2(34)
C(21)	0.333 9(26)	−0.223 9(25)	0.183 7(47)	C(82)	−0.017 5(31)	−0.211 6(30)	0.241 7(56)
O(21)	0.393 4(19)	−0.207 5(19)	0.167 6(35)	O(82)	−0.066 4(26)	−0.235 0(26)	0.304 5(49)
C(22)	0.257 9(22)	−0.327 4(22)	−0.032 7(42)	C(91)	−0.014 7(25)	−0.388 3(26)	−0.176 1(48)
O(22)	0.271 5(20)	−0.374 0(20)	−0.100 2(37)	O(91)	−0.020 0(17)	−0.439 4(17)	−0.241 8(32)
C(31)	0.245 9(27)	−0.025 9(28)	−0.050 2(52)	C(92)	−0.094 3(35)	−0.349 2(34)	0.000 1(66)
O(31)	0.260 1(17)	0.025 7(18)	−0.124 1(33)	O(92)	−0.155 2(20)	−0.372 6(20)	0.073 1(38)
C(32)	0.296 6(21)	−0.059 8(21)	0.163 0(38)	C(93)	−0.038 6(28)	−0.260 4(29)	−0.198 3(54)
O(32)	0.342 3(19)	−0.030 2(19)	0.215 5(36)	O(93)	−0.055 1(23)	−0.229 4(23)	−0.280 6(44)
C(41)	0.130 0(25)	−0.158 1(26)	−0.216 8(47)	C(101)	0.086 1(21)	−0.413 6(21)	0.013 9(39)
O(41)	0.120 1(18)	−0.112 7(18)	−0.283 3(34)	O(101)	0.087 4(16)	−0.465 8(16)	−0.053 7(30)
C(42)	0.159 4(22)	−0.286 2(23)	−0.240 1(42)	C(102)	−0.000 3(23)	−0.382 7(23)	0.216 2(42)
O(42)	0.165 3(20)	−0.335 7(21)	−0.318 1(39)	O(102)	−0.051 0(18)	−0.414 4(18)	0.270 3(33)

Table 8. Fractional atomic co-ordinates for $[Os_{10}C(CO)_{24}(\mu\text{-}I)_2]$ (**3**)

Atom	*x*	*y*	*z*	Atom	*x*	*y*	*z*
Os(1)	0.031 6(1)	−0.380 2(2)	0.021 1(2)	C(51)	0.065 6(26)	0.126 4(68)	0.012 4(74)
Os(2)	0.071 6(1)	−0.181 2(2)	0.042 2(2)	O(51)	0.036 6(21)	0.166 1(55)	−0.025 9(59)
Os(3)	0.121 0(1)	−0.375 3(2)	0.038 6(2)	C(52)	0.093 8(20)	0.056 4(54)	0.222 2(57)
Os(4)	0.080 7(1)	−0.298 9(2)	−0.170 3(2)	O(52)	0.083 7(19)	0.048 5(49)	0.319 3(52)
Os(5)	0.108 3(1)	0.019 6(2)	0.071 4(2)	C(53)	0.148 2(23)	0.126 7(65)	0.081 7(65)
Os(6)	0.164 9(1)	−0.163 9(2)	0.067 2(2)	O(53)	0.178 2(27)	0.199 7(70)	0.091 7(71)
Os(7)	0.205 9(1)	−0.454 3(2)	−0.003 5(2)	C(61)	0.204 9(18)	−0.062 0(48)	0.029 9(50)
Os(8)	0.175 9(1)	−0.283 8(2)	−0.145 5(2)	O(61)	0.232 6(13)	0.004 8(36)	0.000 4(39)
Os(9)	0.171 2(1)	−0.137 6(2)	−0.331 1(2)	C(62)	0.159 7(20)	−0.136 8(58)	0.218 1(56)
Os(10)	0.121 1(1)	−0.084 4(2)	−0.135 4(2)	O(62)	0.159 1(15)	−0.117 0(42)	0.318 7(42)
I(1)	0.231 2(1)	−0.292 5(4)	0.143 7(4)	C(71)	0.210 1(19)	−0.551 8(52)	0.107 7(53)
I(2)	0.098 5(1)	−0.250 8(4)	−0.393 9(3)	O(71)	0.212 3(16)	−0.609 3(43)	0.182 8(47)
C	0.124 6(25)	−0.228 0(63)	−0.070 0(68)	C(72)	0.192 8(19)	−0.557 5(52)	−0.098 3(51)
C(11)	0.016 3(22)	−0.516 6(28)	−0.031 2(61)	O(72)	0.177 0(21)	−0.633 9(57)	−0.160 3(58)
O(11)	0.005 5(15)	−0.607 3(43)	−0.045 7(46)	C(73)	0.266 5(27)	−0.479 5(68)	−0.030 7(74)
C(12)	0.018 6(22)	−0.415 9(57)	0.171 7(63)	O(73)	0.298 2(17)	−0.499 8(43)	−0.079 0(48)
O(12)	0.011 5(20)	−0.433 9(52)	0.267 7(58)	C(81)	0.230 8(19)	−0.246 4(50)	−0.135 7(55)
C(13)	−0.028 0(31)	−0.344 1(80)	−0.001 7(88)	O(81)	0.269 4(13)	−0.218 1(35)	−0.130 9(38)
O(13)	−0.061 9(17)	−0.307 8(44)	−0.035 9(47)	C(82)	0.180 7(27)	−0.375 7(71)	−0.242 1(73)
C(21)	0.052 5(23)	−0.185 5(61)	0.193 7(63)	O(82)	0.185 7(16)	−0.442 2(45)	−0.319 3(50)
O(21)	0.052 4(19)	−0.187 2(49)	0.285 7(53)	C(91)	0.159 7(18)	−0.019 7(52)	−0.418 8(53)
C(22)	0.018 8(21)	−0.107 4(55)	0.016 3(60)	O(91)	0.149 0(19)	0.058 8(54)	−0.471 3(58)
O(22)	−0.011 5(17)	−0.060 2(45)	−0.017 7(50)	C(92)	0.216 9(19)	−0.063 8(52)	−0.280 5(53)
C(31)	0.106 2(32)	−0.542 0(86)	0.007 6(97)	O(92)	0.250 6(17)	−0.015 6(46)	−0.248 4(45)
O(31)	0.104 7(18)	−0.623 8(51)	−0.001 5(56)	C(93)	0.200 4(27)	−0.213 0(70)	−0.453 4(78)
C(32)	0.122 5(23)	−0.389 3(59)	0.191 4(61)	O(93)	0.226 1(23)	−0.246 8(59)	−0.533 4(65)
O(32)	0.125 4(20)	−0.383 4(51)	0.302 9(52)	C(101)	0.150 9(25)	0.038 7(72)	−0.179 1(78)
C(41)	0.021 9(27)	−0.270 4(71)	−0.204 9(72)	O(101)	0.162 7(16)	0.134 7(49)	−0.177 9(46)
O(41)	−0.015 7(18)	−0.227 7(47)	−0.238 3(48)	C(102)	0.076 6(19)	−0.030 3(50)	−0.219 3(51)
C(42)	0.080 3(26)	−0.441 6(71)	−0.239 6(71)	O(102)	0.043 7(18)	0.008 0(45)	−0.261 8(47)
O(42)	0.075 2(17)	−0.536 9(47)	−0.242 0(46)				

Table 9. Fractional atomic co-ordinates for the anion in $[N(PPh_3)_2]_2[Os_{10}C(CO)_{22}(NO)I]$ (**4**)

Atom	*x*	*y*	*z*
Os(1)	0.351 0(1)	0.149 5(1)	−0.137 4(2)
Os(2)	0.318 0(1)	0.250 6(1)	0.058 4(2)
Os(3)	0.250 3(1)	0.202 2(1)	−0.177 2(2)
Os(4)	0.288 1(1)	0.094 7(1)	0.007 8(2)
Os(5)	0.282 3(1)	0.348 3(1)	0.254 6(2)
Os(6)	0.215 2(1)	0.305 5(1)	0.026 3(2)
Os(7)	0.151 2(1)	0.254 6(1)	−0.200 8(2)
Os(8)	0.185 4(1)	0.148 4(1)	−0.022 8(2)
Os(9)	0.226 3(1)	0.047 3(1)	0.163 7(2)
Os(10)	0.253 2(1)	0.198 5(1)	0.213 5(2)
I(1)	0.059 5(4)	0.295 7(5)	−0.133 9(10)
I(2)	0.306 0(4)	0.494 9(5)	0.227 1(10)
C	0.248 3(16)	0.197 9(23)	0.024 4(41)
C(11)	0.375 2(22)	0.213 9(33)	−0.224 3(56)
O(11)	0.395 6(17)	0.265 1(25)	−0.256 0(45)
C(12)	0.351 7(22)	0.072 6(33)	−0.280 7(59)
O(12)	0.349 2(15)	0.020 8(22)	−0.361 3(41)
C(13)	0.415 6(10)	0.118 5(34)	−0.047 4(55)
O(13)	0.455 9(6)	0.097 4(21)	0.003 7(36)
C(21)	0.340 6(21)	0.329 4(31)	0.005 8(55)
O(21)	0.357 2(13)	0.387 5(20)	−0.029 2(35)
C(22)	0.373 8(31)	0.236 0(45)	0.177 4(84)
O(22)	0.408 5(16)	0.200 2(23)	0.240 9(42)
C(31)	0.271 4(20)	0.276 2(29)	−0.276 5(52)
O(31)	0.275 7(13)	0.317 5(19)	−0.344 8(35)
C(32)	0.234 7(16)	0.135 5(25)	−0.313 1(43)
O(32)	0.229 6(12)	0.083 5(18)	−0.411 4(33)
C(41)	0.277 0(20)	0.009 3(31)	−0.106 1(55)
O(41)	0.270 0(16)	−0.048 5(24)	−0.174 4(43)
C(42)	0.344 (27)	0.043 7(38)	0.095 2(73)
O(42)	0.378 7(20)	0.027 6(28)	0.171 6(53)
C(51)	0.237 7(25)	0.385 2(36)	0.360 9(66)
O(51)	0.208 5(15)	0.412 8(22)	0.427 8(40)
C(52)	0.338 1(19)	0.340 5(27)	0.397 2(50)
O(52)	0.372 3(15)	0.328 3(21)	0.472 1(41)
C(53)	0.300 90	0.447 80	0.222 00
C(61)	0.220 1(19)	0.397 5(29)	−0.019 0(51)
O(61)	0.229 0(15)	0.453 7(22)	−0.077 2(40)
C(62)	0.166 8(17)	0.349 1(24)	0.097 5(44)
O(62)	0.128 6(15)	0.370 4(22)	0.146 3(40)
C(71)	0.155 8(18)	0.338 3(27)	−0.286 9(48)
O(71)	0.164 0(14)	0.388 8(21)	−0.337 4(37)
C(72)	0.124 2(21)	0.194 5(30)	−0.333 5(57)
O(72)	0.110 1(13)	0.149 7(20)	−0.432 3(27)
C(73)	0.095 40	0.299 60	−0.164 20
C(81)	0.163 8(20)	0.065 9(31)	−0.141 2(56)
O(81)	0.146 5(15)	0.023 4(22)	−0.221 6(41)
C(82)	0.125 8(28)	0.151 0(40)	0.041 7(73)
O(82)	0.093 0(16)	0.170 9(23)	0.090 5(42)
C(91)	0.205 4(24)	−0.050 0(38)	0.068 2(65)
O(91)	0.195 3(14)	−0.103 3(23)	0.011 4(40)
C(92)	0.269 3(24)	0.000 4(35)	0.292 2(63)
O(92)	0.302 4(19)	−0.037 5(28)	0.338 6(50)
C(93)	0.178 4(24)	0.045 6(33)	0.253 6(63)
O(93)	0.140 4(16)	0.056 8(23)	0.313 8(43)
C(101)	0.202 7(24)	0.218 7(34)	0.328 6(63)
O(101)	0.180 1(16)	0.235 5(23)	0.399 5(43)
C(102)	0.302 5(26)	0.164 8(37)	0.353 8(71)
O(102)	0.332 4(17)	0.151 9(24)	0.440 1(46)

Table 10. Fractional atomic co-ordinates for $[Os_{10}C(CO)_{21}\{P(OMe)_3\}_4]$ (**6**)

Atom	*x*	*y*	*z*
Os(9)	0.839 27(8)	0.339 27(8)	0.25
Os(3)	0.75	0.421 45(12)	0.064 14(19)
Os(8)	0.75	0.25	0.066 35(24)
P(3)	0.75	0.558 4(8)	0.098 4(13)
C	0.75	0.25	0.25
O(34)	0.75	0.613 2(28)	−0.015 7(37)
C(34)	0.75	0.685 2(44)	−0.066 4(99)
C(34a)	0.798 7(90)	0.626 2(99)	−0.107 0(99)
O(35)	0.680 2(21)	0.604 2(21)	0.170 8(29)
C(35)	0.602 9(29)	0.597 8(44)	0.143 3(56)
C(91)	0.924 5(25)	0.353 2(27)	0.152 8(35)
O(91)	0.982 8(23)	0.367 2(23)	0.093 6(31)
C(31)	0.672 3(28)	0.433 1(29)	−0.051 4(41)
O(31)	0.621 1(24)	0.446 7(23)	−0.120 4(31)
C(81)	0.672 9(28)	0.25	−0.051 3(45)
O(81)	0.619 7(24)	0.25	−0.127 1(32)
C(39)	0.75	0.457 2(15)	0.239 0(20)
O(39)	0.75	0.501 3(77)	0.331 6(82)

equiv.) were stirred together in acetone, CH_2Cl_2, or tetrahydrofuran, total conversion to the monoanion $[Os_{10}C(CO)_{24}(\mu\text{-}I)]^-$ was observed.

(*d*) L = CO. Compound (**3**) (100 mg, 0.035 mmol) was heated in CH_2Cl_2 (5 cm^3) in an autoclave for 5 h at 175 °C under a working pressure of 57.5 atm of CO. The product mixture was chromatographed on silica plates using acetone–hexane (1:1) as eluant to give in order of decreasing R_f value, $[Os_{10}C(CO)_{24}(\mu\text{-}I)]^-$, $[Os_{10}C(CO)_{24}]^{2-}$, and a brown baseline that could not be extracted from the silica.

(*e*) L = $[NO_2]^-$ (*in* CH_2Cl_2). Complex (**3**) (30 mg, 0.01 mmol) was dissolved in CH_2Cl_2 (5 cm^3) and 1 mol equiv. of $[N(PPh_3)_2][NO_2]$ (6.2 mg) was added as a solid. The mixture was stirred for 6 h at room temperature and then chromatographed on silica plates using CH_2Cl_2 as eluant to give three products (in order of decreasing R_f): compound (**4b**), purple-red (60%); compound (**4a**), olive green (10%); and $[N(PPh_3)_2]_2[Os_{10}C(CO)_{22}(NO)I]$ (**4**) (20%). The i.r. spectra are listed in Table 2. Attempts to obtain crystals of (**4a**) and (**4b**) from CH_2Cl_2–Pr^{i}OH gave in both cases a quantitative yield of compound (**4**).

Preparation of $[N(PPh_3)_2]_2[Os_{10}C(CO)_{22}(NO)I]$ (**4**).—Complex (**3**) (60 mg, 0.021 mmol) was dissolved in CH_2Cl_2 (10 cm^3) and excess $[N(PPh_3)_2][NO_2]$ (50 mg, 0.086 mmol) was added as a solid. The mixture was stirred for 6 h at room temperature. This gave (**4**) as the major product after separation by t.l.c. using acetone–hexane (1:1) as eluant and crystallisation from CH_2Cl_2–Pr^{i}OH, yield 51 mg, 64% (Found: C, 29.8; H, 1.60; N, 1.00. Calc. for $C_{95}H_{60}IN_3O_{23}Os_{10}$: C, 30.3: H, 1.60; N, 1.10%). Compound (**4**) was characterised by *X*-ray structure determination.

Reaction of $[N(PPh_3)_2][Os_{10}C(CO)_{24}(\mu\text{-}I)]$ (**2**) *with Excess* $[N(PPh_3)_2][NO_2]$.—The compound $[N(PPh_3)_2][Os_{10}C(CO)_{24}(\mu\text{-}I)]$ (60 mg, 0.018 mmol) was dissolved in CH_2Cl_2 (10 cm^3) and excess $[N(PPh_3)_2][NO_2]$ (50 mg, 0.086 mmol) was added as a solid. The mixture was stirred for 6 h at room temperature. Separation of the mixture by t.l.c. using CH_2Cl_2 as eluant gave (in order of decreasing R_f) unreacted $[N(PPh_3)_2][Os_{10}C(CO)_{24}(\mu\text{-}I)]$ (**2**) (65%) and $[N(PPh_3)_2]_2[Os_{10}C(CO)_{24}]$ (**1**) (25%), and these were crystallised from CH_2Cl_2–MeOH and characterised by i.r. spectroscopy.

Reaction of $[Os_{10}C(CO)_{24}(\mu\text{-}I)_2]$ (**3**) *with* $P(OMe)_3$ *in Toluene and Xylene.*—Complex (**3**) was heated under reflux in

Table 11. Fractional atomic co-ordinates for $[Os_{10}C(CO)_{21}\{P(OMe)_3\}_4]$ (**6a**)

Atom	*x*	*y*	*z*	Atom	*x*	*y*	*z*
Os(1)	0.377 96(6)	0.043 13(11)	0.138 52(11)	O(34)	0.402 3(13)	0.573 1(25)	−0.253 4(25)
Os(2)	0.121 54(5)	0.060 99(11)	−0.133 07(10)	C(34)	0.434 9(19)	0.526 7(36)	−0.341 5(36)
Os(3)	0.308 39(6)	0.374 25(11)	−0.202 84(11)	O(35)	0.282 7(13)	0.578 3(24)	−0.357 0(24)
Os(4)	0.211 17(6)	0.365 34(11)	0.231 75(10)	C(35)	0.285 5(23)	0.689 8(44)	−0.400 7(43)
Os(5)	0.299 43(5)	0.208 35(11)	0.180 02(10)	C(41)	0.271 3(15)	0.453 1(27)	0.330 6(27)
Os(6)	0.166 04(5)	0.226 10(11)	0.035 96(10)	O(41)	0.313 9(13)	0.504 9(23)	0.395 3(23)
Os(7)	0.215 71(6)	0.217 15(11)	−0.184 08(10)	C(42)	0.188 1(14)	0.309 8(27)	0.363 5(27)
Os(8)	0.351 63(5)	0.216 92(11)	−0.037 74(10)	O(42)	0.168 4(11)	0.271 5(21)	0.444 9(21)
Os(9)	0.265 84(6)	0.379 96(11)	0.020 73(10)	O(43)	0.129 0(13)	0.511 7(25)	0.376 5(25)
Os(10)	0.254 25(5)	0.059 81(11)	−0.014 30(10)	C(43)	0.087 1(24)	0.591 4(45)	0.416 5(44)
P(1)	0.378 2(4)	−0.093 0(8)	0.256 8(8)	O(44)	0.154 6(14)	0.598 0(27)	0.191 1(27)
P(2)	0.107 9(4)	−0.054 1(8)	−0.295 8(7)	C(44)	0.111 7(23)	0.693 6(45)	0.146 3(44)
P(3)	0.331 6(5)	0.545 0(9)	−0.240 5(9)	O(45)	0.062 0(12)	0.486 4(23)	0.160 7(23)
P(4)	0.135 0(4)	0.493 1(9)	0.234 0(8)	C(45)	0.016 6(23)	0.403 5(41)	0.198 0(42)
C	0.260 5(11)	0.222 1(21)	−0.001 9(20)	C(51)	0.365 6(15)	0.271 5(28)	0.292 3(28)
C(11)	0.455 8(16)	0.091 6(30)	0.243 2(30)	O(51)	0.409 5(11)	0.312 5(21)	0.364 1(21)
O(11)	0.507 2(13)	0.118 5(24)	0.311 5(24)	C(52)	0.267 5(13)	0.128 4(25)	0.289 8(24)
C(12)	0.423 3(14)	−0.048 4(26)	0.048 0(25)	O(52)	0.242 9(11)	0.087 1(21)	0.357 2(21)
O(12)	0.452 1(10)	−0.096 8(18)	−0.011 4(18)	C(61)	0.096 2(15)	0.311 6(28)	−0.030 1(28)
O(13)	0.354 9(12)	−0.083 3(23)	0.383 0(23)	O(61)	0.053 7(12)	0.363 0(23)	−0.080 4(23)
C(13)	0.387 0(19)	0.001 8(35)	0.481 7(35)	C(62)	0.119 2(15)	0.146 6(28)	0.134 5(28)
O(14)	0.451 1(12)	−0.137 7(22)	0.295 2(22)	O(62)	0.088 6(11)	0.114 4(20)	0.193 7(20)
C(14)	0.470 4(24)	−0.228 1(45)	0.362 1(44)	C(71)	0.244 3(13)	0.134 6(24)	−0.301 0(24)
O(15)	0.335 5(11)	−0.190 4(21)	0.192 1(21)	O(71)	0.260 9(10)	0.080 3(20)	−0.372 4(20)
C(15)	0.303 0(21)	−0.261 8(39)	0.264 9(39)	C(72)	0.135 2(15)	0.241 7(27)	−0.281 8(27)
C(21)	0.037 9(13)	0.115 2(25)	−0.198 7(25)	O(72)	0.085 5(11)	0.267 4(20)	−0.342 2(20)
O(21)	−0.014 3(11)	0.147 4(21)	−0.238 2(21)	C(81)	0.389 9(12)	0.127 8(23)	−0.140 3(22)
C(22)	0.081 9(12)	−0.035 6(23)	−0.058 1(23)	O(81)	0.413 5(10)	0.080 4(19)	−0.207 7(19)
O(22)	0.053 6(11)	−0.093 6(20)	−0.009 1(20)	C(82)	0.432 8(14)	0.251 9(26)	0.066 8(26)
O(23)	0.032 4(10)	−0.091 5(19)	−0.322 9(19)	O(82)	0.481 5(11)	0.283 8(21)	0.130 4(21)
C(23)	0.006 1(18)	−0.171 7(34)	−0.422 7(34)	C(91)	0.334 4(16)	0.469 0(29)	0.105 3(29)
O(24)	0.117 5(10)	0.003 6(19)	−0.415 2(19)	O(91)	0.382 2(13)	0.510 7(24)	0.158 6(24)
C(24)	0.135 1(18)	−0.051 8(33)	−0.523 8(33)	C(92)	0.210 4(16)	0.493 4(30)	−0.022 8(30)
O(25)	0.152 3(11)	−0.157 7(20)	−0.294 9(20)	O(92)	0.173 4(15)	0.558 5(27)	−0.055 3(26)
C(25)	0.153 9(20)	−0.234 0(37)	−0.197 6(37)	C(101)	0.282 1(14)	−0.043 7(26)	−0.113 9(26)
C(31)	0.323 4(15)	0.320 7(27)	−0.349 3(28)	O(101)	0.298 5(12)	−0.107 5(22)	−0.178 3(22)
O(31)	0.331 5(13)	0.287 0(24)	−0.441 7(25)	C(102)	0.221 7(15)	−0.031 1(28)	0.075 6(27)
C(32)	0.217 9(19)	0.409 7(33)	−0.268 6(33)	O(102)	0.198 5(11)	−0.086 2(21)	0.140 2(21)
O(32)	0.170 3(14)	0.454 2(26)	−0.309 3(26)	C(38)	0.403 8(25)	0.364 5(44)	−0.118 8(46)
O(33)	0.321 8(14)	0.635 8(26)	−0.142 6(27)	O(38)	0.460 3(17)	0.387 7(29)	−0.094 2(29)
C(33)	0.374 6(23)	0.685 8(41)	−0.054 2(43)				

toluene for 4 h with one drop of $P(OMe)_3$; no reaction was observed under these conditions. In xylene, however, on treatment of (**3**) (100 mg, 0.035 mmol) with $P(OMe)_3$ (2 drops) under reflux for 3.5 h reaction was complete, as monitored by t.l.c. and i.r. spectroscopy. Removal of the solvent under reduced pressure gave a black residue which was extracted into CH_2Cl_2 and separation by t.l.c. using CH_2Cl_2–hexane (2:1) as eluant gave five main bands. Band 1 was separated by a second t.l.c. [ethyl acetate–hexane (6:4)] into two components, (*i*) brown crystals of (**6**), characterised by an *X*-ray analysis, and (*ii*) yellow crystals of compound (**7**). Band 2 could not be further separated or characterised. Band 3 was shown to consist of a single compound, reddish brown (**8**). Band 4 was separated by a second t.l.c. [ethyl acetate–hexane (7.5:2.5)] into two components, (*i*) yellow crystals of (**9**) and green crystals of (**10**). Band 5 was shown to be pure and crystallised as dark brown crystals of (**5**), which were characterised by an *X*-ray structure determination. The i.r. spectra of compounds (**5**)—(**10**) are given in Table 2.

Reaction of $[Os_{10}C(CO)_{23}\{P(OMe)_3\}(\mu\text{-}I)_2]$ (**5**) *and Complex* (**8**) *with Iodide Ion.*—Compounds (**5**) and (**7**) (2 mg) were dissolved in turn in acetone (0.5 cm³) and a dilute solution of $[NBu_4]I$, in acetone, was added. The reaction was monitored by i.r. spectroscopy. For compound (**5**), sequential dissociation of 'I^+' was seen to give the monoanion $[Os_{10}C(CO)_{23}\{P(OMe)_3\}(\mu\text{-}I)]^-$ (**5a**) followed by formation of the dianion $[Os_{10}C(CO)_{23}\{P(OMe)_3\}]^{2-}$ (**5b**). For (**8**) only a monoanion, complex (**8a**), was observed by i.r. spectroscopy (see Table 2).

Reaction of $[Os_{10}H_2C(CO)_{24}]$ *with* $P(OMe)_3$ *in Xylene.*—Excess $P(OMe)_3$ was added to a solution/suspension of $[Os_{10}H_2C(CO)_{24}]$ (50 mg, 0.014 mmol) in refluxing xylene. After 2 h the reaction mixture was cooled to leave a cloudy, dark red solution. The solvent was removed under vacuum and the dichloromethane-soluble residue chromatographed on thin silica plates using ethyl acetate–hexane (4:1) as eluant to give five bands. Complex $[Os_{10}C(CO)_{21}\{P(OMe)_3\}_4]$ (**6a**), obtained as red crystals (R_f 0.60), was the main product of the reaction.

X-*Ray Structure Analyses.*—Single crystals of (**2**), (**3**), (**4**), (**5**), (**6**), and (**6a**) suitable for *X*-ray analysis were grown over a period of days at room temperature using the slow evaporation technique. Unit-cell determinations and data collection were carried out using a PW 1100 four-circle diffractometer by the techniques previously described.[12] Details of the parameters of

Table 12. Fractional atomic co-ordinates for $[Os_{10}C(CO)_{23}\{P(OMe)_3\}(\mu\text{-}I)_2]\cdot CH_2Cl_2$ (**5**)

Atom	*x*	*y*	*z*	Atom	*x*	*y*	*z*
Os(1)	0.042 89(8)	0.086 53(8)	0.298 71(17)	C(42)	−0.062 8(21)	0.122 0(22)	0.405 7(46)
Os(2)	−0.035 49(7)	0.151 07(8)	0.121 36(16)	O(42)	−0.087 0(14)	0.077 3(14)	0.444 4(29)
Os(3)	0.067 79(7)	0.218 24(8)	0.223 33(16)	C(51)	−0.102 2(18)	0.156 3(19)	−0.190 7(40)
Os(4)	−0.019 86(7)	0.201 55(7)	0.370 25(16)	O(51)	−0.091 8(15)	0.125 9(15)	−0.279 9(33)
Os(5)	−0.114 67(8)	0.210 05(9)	−0.061 55(17)	C(52)	−0.154 1(20)	0.277 2(22)	−0.162 9(46)
Os(6)	−0.014 47(7)	0.287 96(8)	0.030 56(16)	O(52)	−0.179 8(17)	0.316 1(18)	−0.229 9(37)
Os(7)	0.119 00(8)	0.351 58(9)	0.258 41(18)	C(53)	−0.179 7(18)	0.157 6(19)	−0.053 5(39)
Os(8)	0.004 19(7)	0.340 55(8)	0.283 90(17)	O(53)	−0.219 4(17)	0.125 9(17)	−0.048 3(35)
Os(9)	−0.105 92(7)	0.377 92(8)	0.338 50(18)	C(61)	0.002 1(21)	0.248 3(21)	−0.120 3(47)
Os(10)	−0.103 24(7)	0.266 01(8)	0.170 15(16)	O(61)	0.012 4(16)	0.224 2(17)	−0.207 8(37)
I(1)	0.077 2(1)	0.369 6(2)	0.013 7(3)	C(62)	−0.055 7(18)	0.363 6(20)	−0.035 1(40)
I(2)	−0.086 4(1)	0.271 8(1)	0.505 9(3)	O(62)	−0.080 3(14)	0.411 9(15)	−0.065 9(31)
P	−0.197 7(5)	0.385 7(6)	0.360 2(12)	C(71)	0.186 9(21)	0.319 2(22)	0.229 4(45)
O(1)	−0.236 4(13)	0.322 4(13)	0.301 0(28)	O(71)	0.230 9(16)	0.299 0(17)	0.205 5(34)
C(1)	−0.298 8(27)	0.319 5(28)	0.247 7(58)	C(72)	0.142 8(19)	0.339 1(20)	0.420 8(43)
O(2)	−0.235 7(14)	0.449 8(14)	0.300 8(29)	O(72)	0.159 2(14)	0.334 5(15)	0.528 3(33)
C(2)	−0.219 6(24)	0.520 7(27)	0.348 1(55)	C(73)	0.144 3(22)	0.448 6(24)	0.275 7(48)
O(3)	−0.200 8(13)	0.388 5(14)	0.502 3(29)	O(73)	0.155 2(14)	0.504 5(15)	0.277 2(30)
C(3)	−0.259 9(32)	0.387 1(32)	0.544 3(69)	C(81)	0.001 7(20)	0.433 2(21)	0.221 4(44)
C	−0.015 4(14)	0.246 8(14)	0.208 7(30)	O(81)	0.003 9(13)	0.490 0(14)	0.191 9(28)
C(11)	0.086 5(20)	0.038 4(21)	0.201 1(44)	C(82)	0.027 3(19)	0.359 4(20)	0.452 5(43)
O(11)	0.114 8(18)	0.014 6(19)	0.134 9(40)	O(82)	0.041 9(14)	0.380 9(15)	0.546 3(32)
C(12)	0.092 1(18)	0.070 3(18)	0.445 8(39)	C(91)	−0.114 5(21)	0.447 3(22)	0.225 3(45)
O(12)	0.131 1(14)	0.062 7(14)	0.529 2(31)	O(91)	−0.124 5(16)	0.493 8(17)	0.152 1(35)
C(13)	−0.001 3(19)	0.002 2(20)	0.314 2(40)	C(92)	−0.088 6(21)	0.445 8(22)	0.468 6(48)
O(13)	−0.022 8(14)	−0.045 2(15)	0.338 8(30)	O(92)	−0.068 0(17)	0.478 6(19)	0.552 2(38)
C(21)	−0.005 2(17)	0.099 1(18)	0.014 9(38)	C(101)	−0.158 4(23)	0.328 3(24)	0.103 5(50)
O(21)	0.015 0(15)	0.071 8(16)	−0.071 6(33)	O(101)	−0.196 8(16)	0.359 2(16)	0.039 7(33)
C(22)	−0.090 4(18)	0.079 2(19)	0.126 6(39)	C(102)	−0.157 0(18)	0.214 3(19)	0.222 6(38)
O(22)	−0.123 5(14)	0.039 9(15)	0.140 8(31)	O(102)	−0.191 8(14)	0.173 5(15)	0.249 2(31)
C(31)	0.103 6(21)	0.195 9(23)	0.091 3(48)	Cl(1)	0.766 8(28)	0.031 4(28)	0.612 0(52)
O(31)	0.124 5(14)	0.175 7(14)	0.019 1(31)	Cl(2)	0.722 0(23)	0.129 8(25)	0.434 9(52)
C(32)	0.135 8(19)	0.203 1(19)	0.339 1(40)	C(Cl)	0.789 3(43)	0.086 0(53)	0.495 5(97)
O(32)	0.175 9(15)	0.186 2(16)	0.400 6(33)	Cl(1′)	0.778 7(26)	0.015 0(27)	0.674 1(49)
C(41)	0.038 2(19)	0.202 4(20)	0.506 8(41)	Cl(2′)	0.745 2(24)	0.095 2(26)	0.466 4(55)
O(41)	0.076 4(14)	0.205 4(14)	0.589 1(30)	C(Cl′)	0.754 3(55)	0.003 7(47)	0.509 8(67)

the crystals, and those for data collection and for refinement are summarised in Table 6. Atomic co-ordinates are given in Tables 7—12.

The data sets were corrected for Lorentz and polarisation factors and for absorption.[12] Neutral atomic scattering factors were employed throughout.[13] The structures were solved by Patterson methods and refined by blocked full-matrix least-squares refinement using the SHELX program.[14] For the $[N(PPh_3)_2]^+$ salts (**2**) and (**4**) the phenyl rings were refined as regular hexagons with a C–C distance of 1.395 Å. The solution and refinement of the structures was straightforward except for those of (**4**) and (**6**).

There is disorder in the dianion $[Os_{10}C(CO)_{22}(NO)I]^{2-}$ (**4**), corresponding to two different cluster orientations of equal occupancy related by a virtual C_2 axis through Os(6)–C–Os(4). The terminal I ligand [I(1) or I(2)] and a carbonyl ligand [CO(53) or CO(73)] interchange sites in the two components of the disorder, but the sites of the osmium atoms and the remaining carbonyl atoms are indistinguishable in the two orientations. The two sites occupied by the disordered I atom were assigned half occupancy by this atom and no allowance was made for the carbonyl O atom. Maxima corresponding to the disordered carbonyl C atom [C(53) and C(73)] were located in a difference Fourier synthesis and these atoms were included in the structure factor calculations with half occupancy, but were not refined. From this structure the terminal mode of nitrosyl bonding is clearly established but the NO ligand could not be distinguished from the CO ligands on the basis of thermal parameters.

The carbido-carbon atom at the centre of the neutral molecule $[Os_{10}C(CO)_{21}\{P(OMe)_3\}_4]$ (**6**) occurs at $\frac{3}{4}$, $\frac{1}{4}$, $\frac{1}{4}$, a site of $\overline{4}2m$ symmetry (*b* Wyckoff notation). Figure 7 is the view of the molecule down the $\overline{4}$ axis, showing the atomic-numbering scheme of the unique atoms, which correspond to the fractional atomic co-ordinates given in Table 10. There are three crystallographically independent osmium atoms; Os(1) lies on a C_2 axis, Os(2) on a mirror plane which bisects the phosphite ligand bonded to it, and Os(3) lies on the intersection of two mirror planes. This highly symmetrical description cannot hold for an isolated molecule, because in the crystal it requires a disordering of the μ_3-carbonyl [CO(39)] over four sites, so that it was assigned $\frac{1}{4}$ occupancy in the refinement. Significantly the C(39) atomic site is only 2.25 Å from the P(2) site, indicating that in an isolated molecule of (**6**) one phosphite ligand, attached to the same tetrahedral Os_4 capping group as the μ_3-CO group, must be displaced slightly. Overall it appears that there is a four-fold disorder of the molecule in the crystal; the μ_3-CO and 'displaced' phosphite ligands occur with $\frac{1}{4}$ occupancy at each of the four symmetry-related capping Os atoms. The high thermal parameters of P(3) are consistent with this model although the P atom of the minor component of the disorder could not be resolved; two maxima [C(34) and C(34a)] were located for the carbon atom of one methoxy group of the phosphite ligand. It is reasonable to conclude that the view of one molecule of (**6**)

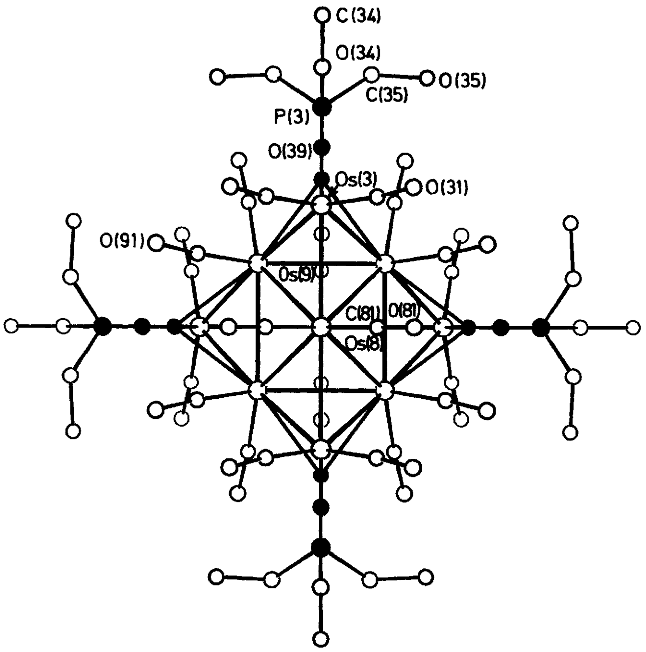

Figure 7. [$Os_{10}C(CO)_{21}\{P(OMe)_3\}_4$], the disordered isomer (**6**), viewed down the $\bar{4}$-fold axis; the numbering of the crystallographically unique atoms corresponding to the atomic co-ordinates given in Table 10

shown in Figure 5(*a*) is substantially correct except in the vicinity of the μ_3-CO ligand where a small displacement of the neighbouring ligands (not resolved in the *X*-ray analysis) must occur. It is important to note that in spite of this slight ambiguity about the exact structure of (**6**) it is clearly established that it is a different isomer from that characterised in the crystal of (**6a**).

Acknowledgements

We thank the S.E.R.C. (D. B., R. J. G., and A. S.), I.C.I. (P. F. J. and W. J. H. N.), CONECIT (Venezuela) (J. P.), and C. N. Pq. (Brazil) (M. D. V.) for financial support.

References

1 J. N. Nicholls, D. H. Farrar, P. F. Jackson, B. F. G. Johnson, and J. Lewis, *J. Chem. Soc., Dalton Trans.*, 1982, 1395.
2 G. R. John, B. F. G. Johnson, and J. Lewis, *J. Organomet. Chem.*, 1979, **169**, C9.
3 P. F. Jackson, B. F. G. Johnson, J. Lewis, W. J. H. Nelson, and M. McPartlin, *J. Chem. Soc., Dalton Trans.*, 1982, 2099.
4 P. F. Jackson, B. F. G. Johnson, J. Lewis, M. McPartlin, and W. J. H. Nelson, *J. Chem. Soc., Chem. Commun.*, 1982, 49.
5 D. Braga, B. F. G. Johnson, J. Lewis, M. McPartlin, W. J. H. Nelson, and M. D. Vargas, *J. Organomet. Chem.*, 1983, **246**, C69.
6 D. Braga, K. Henrick, B. F. G. Johnson, J. Lewis, M. McPartlin, and J. Puga, *J. Chem. Soc., Chem. Commun.*, 1982, 1083; *J. Organomet. Chem.*, 1984, **266**, 173.
7 (*a*) G. R. John, B. F. G. Johnson, J. Lewis, and A. L. Mann, *J. Organomet. Chem.*, 1979, **171**, C9; (*b*) B. F. G. Johnson, J. Lewis, P. R. Raithby, K. Wong, and K. D. Rouse, *J. Chem. Soc., Dalton Trans.*, 1980, 1248; (*c*) A. V. Rivera, M. Sheldrick, and M. B. Hursthouse, *Acta Crystallogr., Sect. B*, 1978, **34**, 3376; (*d*) D. Braga, K. Henrick, B. F. G. Johnson, J. Lewis, M. McPartlin, W. J. H. Nelson, and M. D. Vargas, *J. Chem. Soc., Chem. Commun.*, 1982, 419; D. Braga, B. F. G. Johnson, J. Lewis, M. McPartlin, W. J. H. Nelson, and M. D. Vargas, *J. Organomet. Chem.*, 1983, **249**, C21.
8 C. Eady, B. F. G. Johnson, and J. Lewis, unpublished work.
9 B. F. G. Johnson, J. Lewis, J. Puga, and M. D. Vargas, unpublished work.
10 D. Braga, J. Lewis, B. F. G. Johnson, M. McPartlin, W. J. H. Nelson, and M. D. Vargas, *J. Chem. Soc., Chem. Commun.*, 1983, 241.
11 R. E. Stevens, J. L. Yanta, and W. L. Gladfelter, *J. Am. Chem. Soc.*, 1981, **103**, 4981; D. E. Fjare and W. L. Gladfelter, *Inorg. Chem.*, 1981, **20**, 3533; D. E. Fjare and W. L. Gladfelter, *J. Am. Chem. Soc.*, 1981, **103**, 1572.
12 M. K. Cooper, P. A. Duckworth, K. Henrick, and M. McPartlin, *J. Chem. Soc., Dalton Trans.*, 1981, 2357.
13 'International Tables for *X*-Ray Crystallography,' Kynoch Press, Birmingham, 1974, vol. 4.
14 G. M. Sheldrick, SHELX crystal structure solving package, University of Cambridge, 1976.

Received 16*th November* 1984; *Paper* 4/1947